INFRARED ABSORPTION IN ARSENIC-DOPED SILICON

by

WILLIAM GORUK

A THESIS SUBMITTED IN PARTIAL FULFILMENT OF

THE REQUIREMENTS FOR THE DEGREE OF

MASTER OF SCIENCE

in the Department

of

PHYSICS

We accept this thesis as conforming to the required standard

THE UNIVERSITY OF BRITISH COLUMBIA

July, 1964

In presenting this thesis in partial fulfilment of the requirements for an advanced degree at the University of British Columbia, I agree that the Library shall make it freely available for reference and study. I further agree that permission for extensive copying of this thesis for scholarly purposes may be granted by the Head of my Department or by his representatives. It is understood that copying or publication of this thesis for financial gain shall not be allowed without my written permission.

Department of Physics

The University of British Columbia,
Vancouver 8, Canada

Date July 25/64

ABSTRACT

The optical absorption line $1s_1 - 2p_o$ at the absorption spectrum of arsenic doped silicon has been studied for various arsenic concentrations at four temperatures. The concentrations are $.9 \times 10^{15}$ cm^{-3}, 1.7×10^{15} cm^{-3}, 4.0×10^{15} cm^{-3} and 1.5×10^{16} cm^{-3}, the temperatures are 4.2°K, 53°K, 77°K, and 90°K. Spectrometer broadening was accounted for in the observed line-widths. There was observed two temperature independent broadening mechanisms, concentration and strain broadening. Two temperature dependent broadening mechanisms were observed, phonon broadening and the statistical Stark effect. The five broadening mechanisms are believed to account for the total line-width through the use of the Voigt analysis half-breadth method.

A shift of the peak position with temperature was noted and a possible explanation presented.

ACKNOWLEDGEMENTS

I would like to thank, Dr. J. W. Bichard for his advice during the experimental work and in the preparation of this thesis; and, Professor R. Barrie for aiding in my understanding of the theoretical background of this thesis.

The research for this thesis was supported by the Defence Research Board of Canada, Grant No. 9512-26.

TABLE OF CONTENTS

Page

LIST OF FIGURES

Page

CHAPTER 1

INTRODUCTION

The electron (holes), associated with the unionized group III (group V) impurities in silicon, are optically active. These electrons (holes) will absorb photons in the far infrared region of the electromagnetic spectrum, in making transitions to excited states. The absorption spectrum,thus obtained, resembles in many respects the absorption spectrum of a hydrogen atom imbedded in a dielectric medium.

Investigations of the absorption line-widths in boron doped-silicon have been carried out previously (E. Burstein et al 1956, K. Colbow 1963). Broadening of the line-width was observed and found to be temperature and impurity concentration dependent. It has now been observed that the spectral line-widths of arsenic-doped silicon exhibit similar effects. The line broadening is also temperature and concentration dependent. It is found that the analysis of the line-width broadening can be performed in a manner analagous to that proposed by K. Colbow (1963) for boron-doped silicon absorption lines.

In Chapter I, Section III the effect of finite spectrometer slits is discussed and shown to contribute to the broadening of the observed absorption lines. This is called spectrometer broadening. The effect of the lattice vibrations on the electronic states leads to a "lifetime effect" (Nishikawa and Barrie 1962), which contributes to the broadening. This effect is discussed in Chapter III, Section V, but fails to explain the rapid rise in half-width with temperature. The theory of statistical Stark broadening (K. Colbow 1963) is employed to explain the rapid rise in half-width (Chapter II, Section II) with

temperature. The theory of the statistical Stark broadening (K. Colbow 1963) is employed to explain the rapid rise in half-width (Chapter III Section II) with temperature. There are two broadening mechanisms, which are assumed to be temperature independent, viz., concentration broadening, and strain broadening. The concentration broadening is due to the interaction of neighbouring impurities, and the strain broadening is due to the removal of crystal symmetry by dislocations in the crystal. The theory of W. Baltensperger (1953) is used to describe the concentration broadening (Chapter III, Section 3). The strain broadening is explained in Chapter III, Section 4.

Besides, broadening of the absorption line-width a shift of the centre of the peak with temperature was observed. These results will be presented in Chapter III Section 6.

CHAPTER II

1. Apparatus and Experimental Procedure

A model 83 Perkin Elmer spectrometer, refitted with a Bausch and Lomb grating, was used to disperse the radiation from a globar source. The grating has thirty grooves per millimeter and is blazed at thirty microns in the first order. The theoretical linear dispersion at the exit slits was calculated to be 0.12 microns per millimeter. Experimentally, the resolution of the instrument was observed to be 0.3 microns for one millimeter slits. Second or higher order radiation was limited to less than three per cent of the total signal strength by using sooted mirrors and restrahlen plates of lithium fluoride. Light from the globar was chopped at 13 cycles/sec before the entrance slit of the monochromator. A thermocouple detector was used. The amplified signal was displayed on a Brown strip-chart recorder.

The spectrometer was calibrated with reference to the known atmospheric water vapour absorption spectrum. Data for the water vapour spectrum was taken from L. R. Blaine et al 1962. During an experiment, the spectrometer was flushed with dry nitrogen gas to remove the absorption of the atmospheric water vapour.

A metal dewar, designed for mounting two samples, was used to cool the samples. Either sample could be placed in the light path of the spectrometer by a ninety degree rotation of the sample mount. The dewar consisted of an outer liquid nitrogen jacket and an inner helium container, to which the sample mount was attached. The light beam passed through ports of cesium iodide, which could be removed to allow mounting of the samples.

A wire saw was used to cut samples from silicon ingots of different arsenic dopings. The samples were polished with carborundum abrasive of successively finer grades; the lubricant used was water. A final mirror like finish was obtained by using a cloth covered polishing wheel and a 0.2 micron aluminum oxide suspension in water as the abrasive.

In preparation for a run, the samples were cleaned in a degreasing solution agitated by an ultrasonic viabrator. The final wash was in alcohol. A mixture of silver dust and Apiezon grease was used to make thermal contact to the copper sample mount. The samples were clamped in place carefully to avoid strains. An intrinsic and a doped sample were mounted for the purpose of measuring their relative absorption, from which the absorption coefficient of the doped sample could be determined.

The concentration of the arsenic impurity was determined by room temperature resistivity measurements. The resistivities (and corresponding concentrations of the arsenic impurity) of the five samples used are 0.41Ω-cm. (1.5×10^{16}/cc), 1.3Ω-cm. (4×10^{15}/cc.), 2.8Ω-cm (1.7×10^{15}/cc), 5Ω-cm. ($.9 \times 10^{15}$/cc), and 1,300Ω-cm. (intrinsic). The thickness of the samples varied from .5 cm. for the 5Ω-cm. sample to .003 cm. for the 0.41Ω-cm. sample.

The following liquids at their boiling points were used as coolants; helium 4.2°K, nitrogen 77°K, and oxygen 90°K. A temperature of 53 ± 3°K was achieved by pumping on the liquid nitrogen.

The absorption, due to the $1s_1 - 2p_o$ (Figure 1) transition in arsenic-doped silicon, was studied for the four concentrations and at the four temperatures aforementioned. The absorption in the doped sample was measured relative to the absorption in the intrinsic sample.

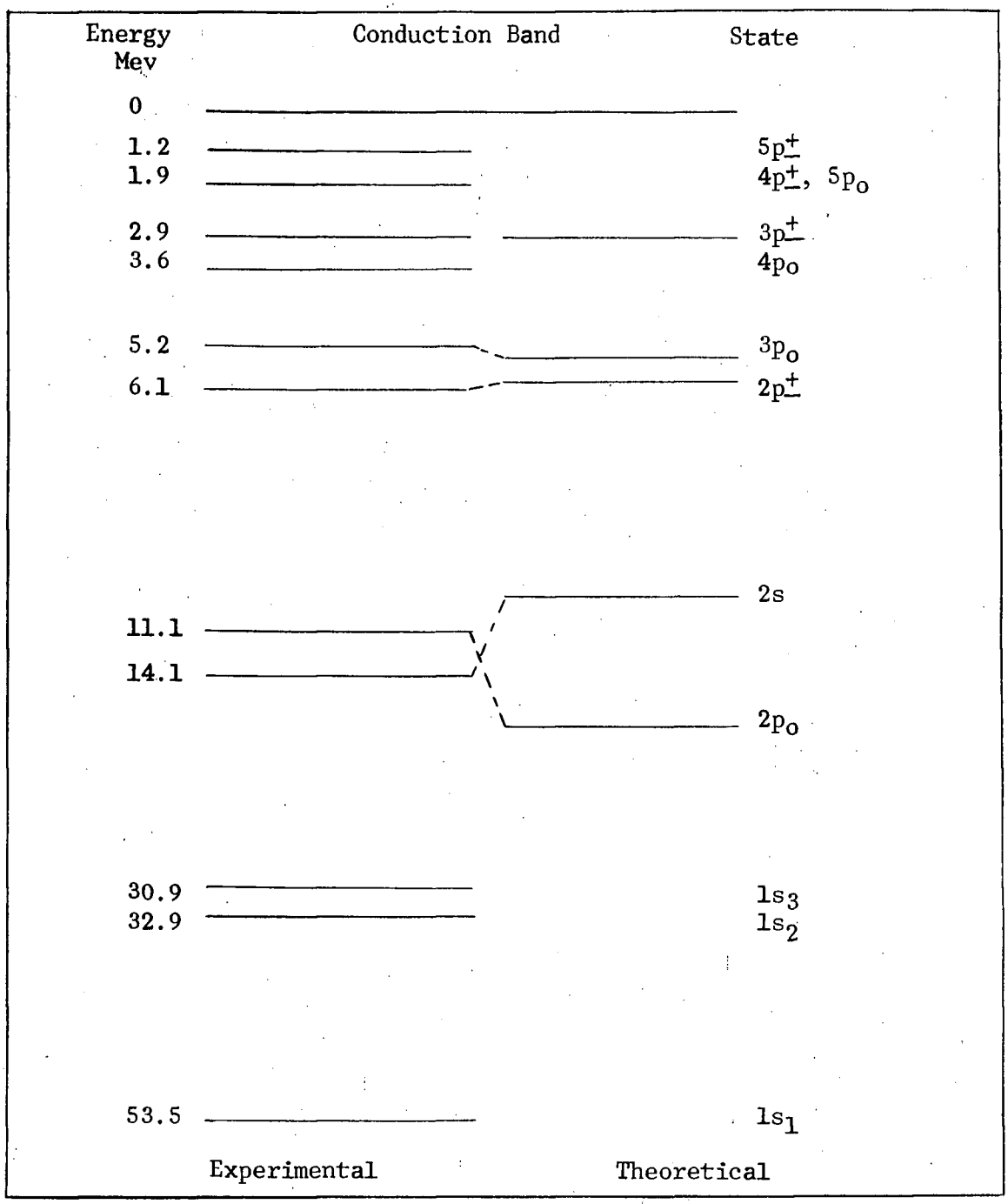

FIG. 1. Energy level diagram for arsenic doped-silicon. Theoretical predictions due to Kohn and Luttinger. Experimental results are due to Bichard and Giles 1962, except for the $1s_2$, $1s_3$ due to P. Ottensmeyer (unpublished) The 2s states are predicted to lie below the $2p_o$ state from experimental evidence.

2. Calculation of the Absorption Coefficient

In general, when interference effects can be neglected, the fractional transmission of monochromatic radiation of wave number k through a specimen of thickness d and surface reflectivity R is

(T.S. Moss 1959)

$$T = \frac{(1-R)^2 \exp(-\alpha d)}{1 - R^2 \exp(-2\alpha d)} \qquad \text{II-1}$$

where $\alpha = \alpha(k)$ is the absorption coefficient at wave number k. For an intrinsic sample ($\alpha = 0$ in the range of k of interest), the transmission becomes

$$T_o = \frac{(1-R)^2}{(1-R^2)} \qquad \text{II-2}$$

Hence, the transmission of a doped sample relative to that of an intrinsic sample is given by

$$\frac{T}{T_o} = \frac{(1-R^2)\exp(-\alpha d)}{1-R^2\exp(-2\alpha d)} \qquad \text{II-3}$$

The surface reflectivity, R was assumed to be the same for both the intrinsic and the arsenic-doped silicon. For the intrinsic sample, using Eq. (II-2), a value of 0.31 ± 0.03 was determined for the reflectivity. This agrees with the value obtained by Bichard and Giles (1962). Within experimental error the reflectivity remained constant over the energy and temperature range studied. Using this value of reflectivity and Eq. (II-3), the graphs of absorption coefficient versus energy of Fig. (2) were obtained for the $1s_1 - 2p_o$ transition.

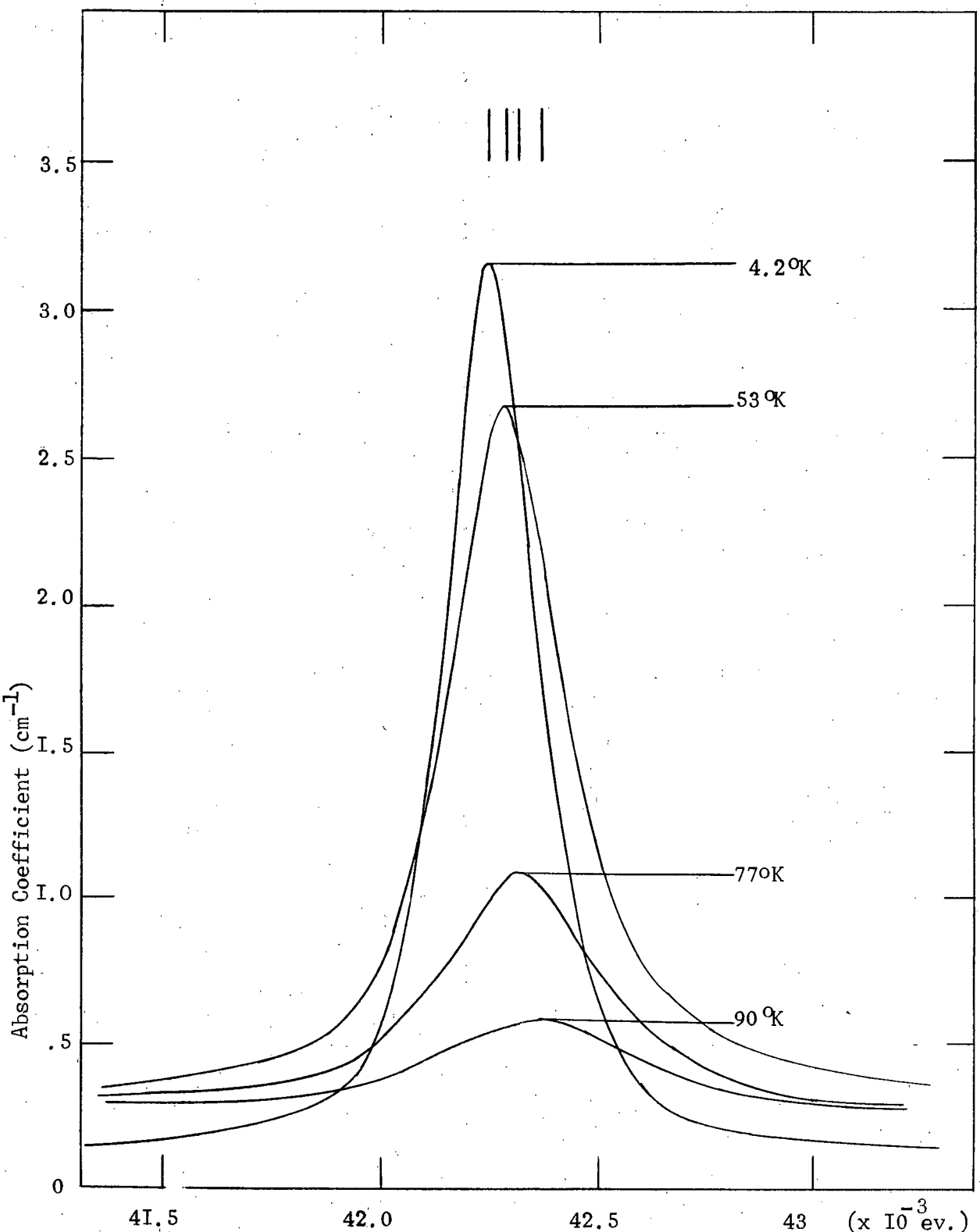

FIG. 2(a). The observed $1s_i$-$2p_0$ absorption of the arsenic-doped silcon, impurity concentration. 9×10^{15}/cc.

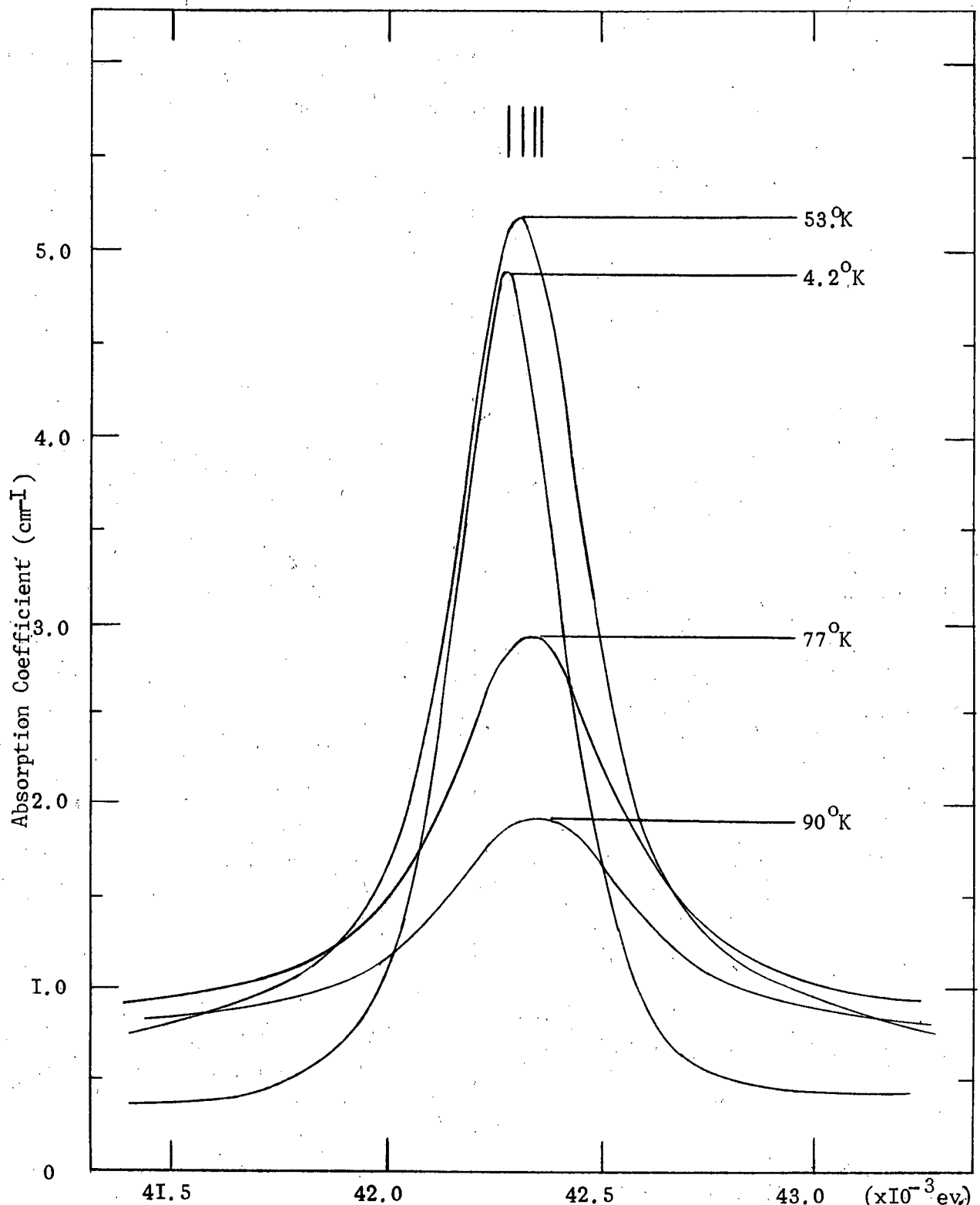

FIG.2(b). The observed $1s_1 - 2p_0$ absorption of the arsenic-doped silicon, impurity concentration 1.7×10^{15}/cc.

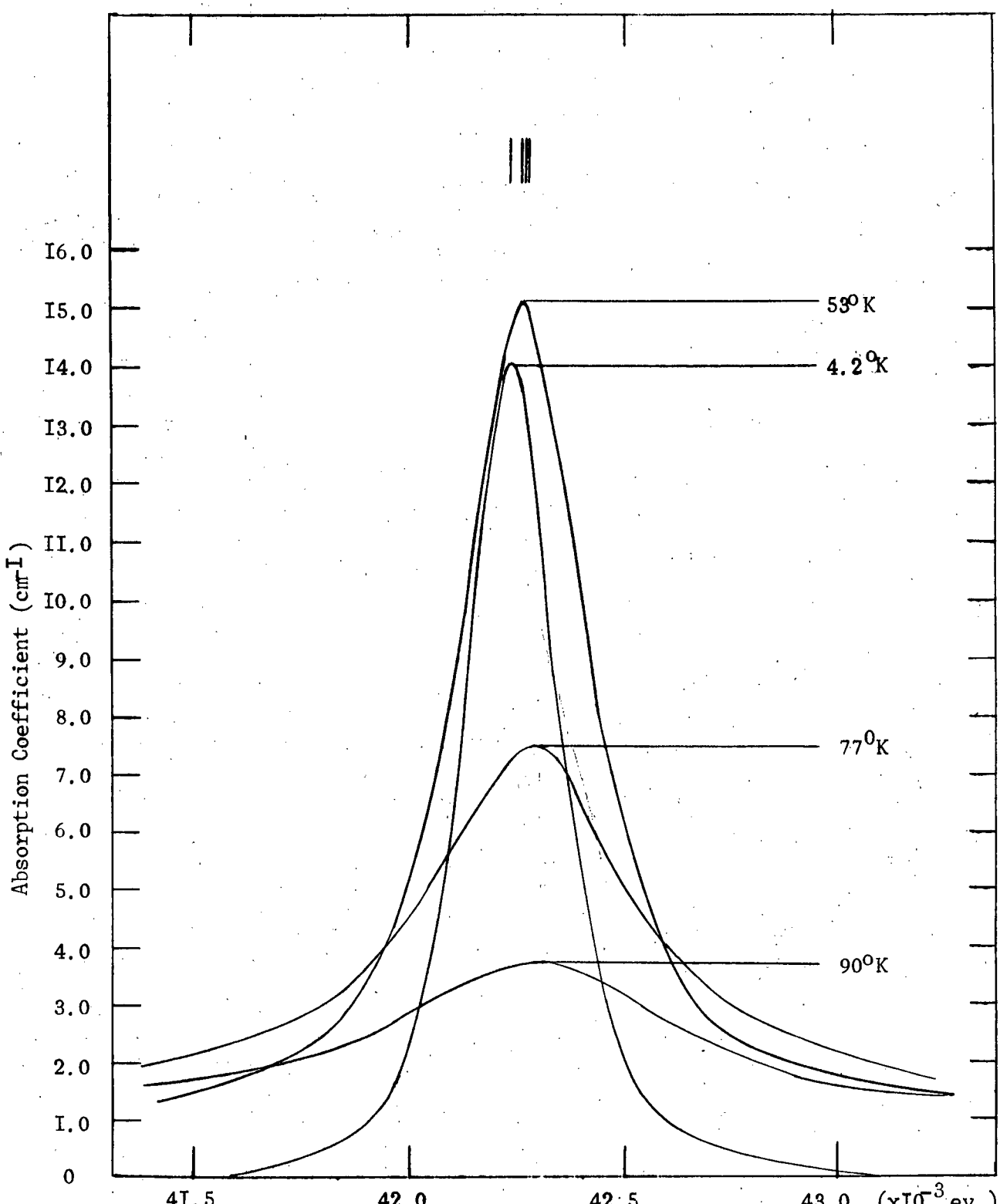

FIG. 2(c). The observed $1s, 2p_{\pm 1}$ absorption of the arsenic-doped silicon, impurity concentration $4.0 \times 10^{}$ /cc.

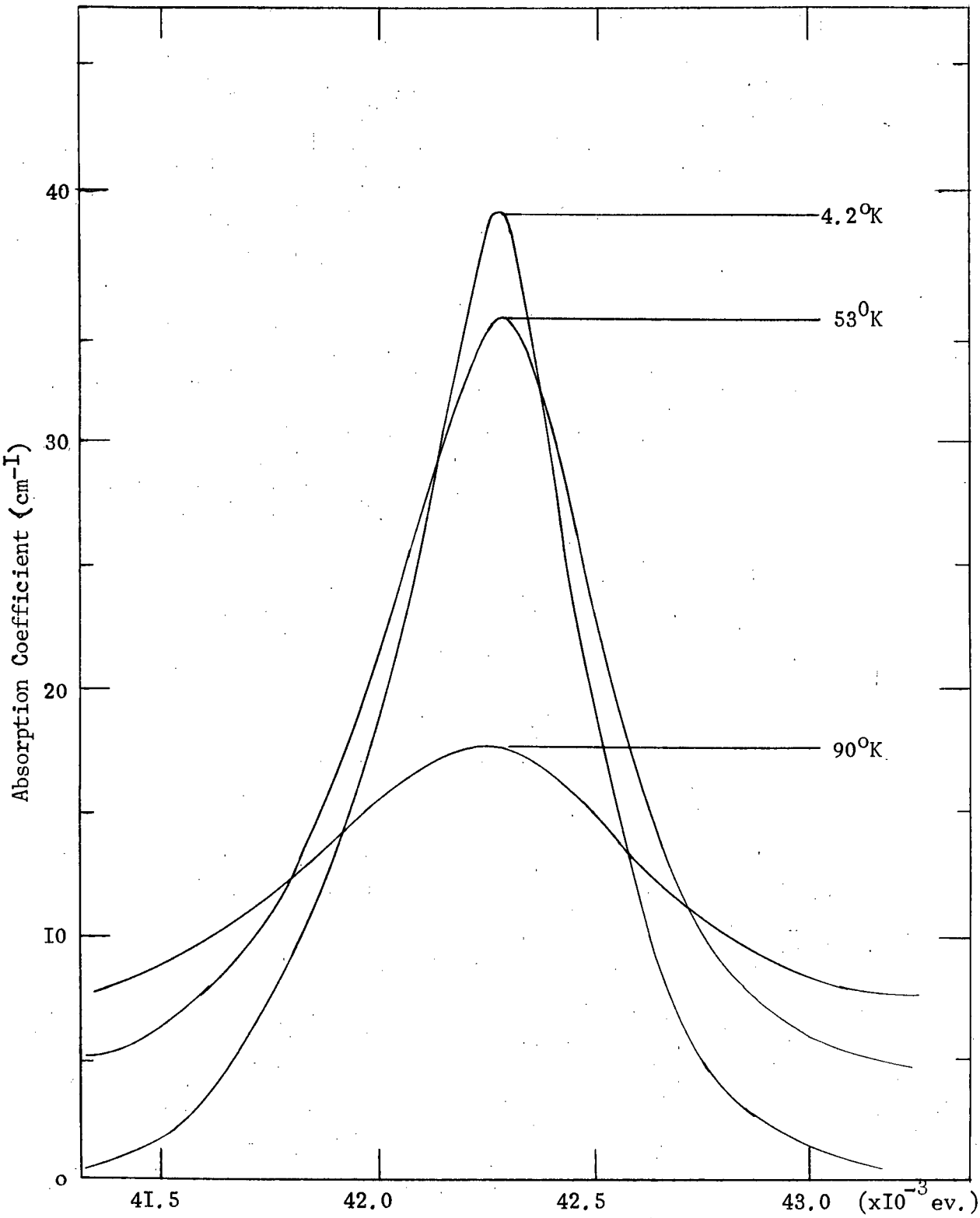

FIG. 2(d). The observed $1s_1 - 2p_0$ absorption of the arsenic-doped silicon, impurity concentration 1.5×10^{16}/cc. .

It should be noted that for some concentrations the 53°K absorption peak has a higher absorption coefficient than the 4.2°K peak. This arises due to the electrons, thermally populating the excited states, being excited to the conduction band, and giving rise to a constant absorption background for the energy range studied. The absorption cross section for the excited states is found to be of the order of 10^{-15} cm^2, consistent with the above interpretation.

3. Spectrometer Broadening

The true shape of the impurity absorption lines is broadened by spectrometer broadening. This is due to the finite width of the spectrometer slits, and is accounted for in the following discussion.

The profile of an absorption line, broadened by two independent effects, is expressed by the convolution integral (Unsöld 1955)

$$f(x) = \int_{-\infty}^{\infty} f'(x-y)\, f''(y)\, dy. \qquad \text{II-4}$$

Here f'(x) and f''(x) are the profiles that the line would assume if only one of the broadening effects was present. All functions f(x), f'(x), and f''(x) denote intensities, and x is the distance from the centre of the line in terms of frequency or wavenumber.

If the profiles f'(x) and f''(x) can be approximated by Gaussian functions, then by Eq. (II-4) f(x) is a Gaussian of the form,

$$f(x) = c\, e^{-x^2/\beta_2^2} \qquad \text{II-5}$$

where C and β_2 are constants. The parameters β_2 , β_2' , and β_2'' are related by the equation,

$$\beta_2^2 = \beta_2'^2 + \beta_2''^2 \qquad \text{II-6}$$

The half-widths for Gaussian functions are equal to 1.665 β_2 and satisfy a similar relation.

Similarly for the functions f' (x), f'' (x) fitted by Lorentzian functions, f(x) will have the form,

$$f(x) = \frac{C}{1 + x^2/\beta_1^2} \qquad \text{II-7}$$

where C and β_1 are constants. The parameters β_1 , β_1' , and β_1'' are related by the equation,

$$\beta_1 = \beta_1' + \beta_1'' \qquad \text{II-8}$$

The half-widths, which for Lorentzian functions are equal to 2 β_1 , satisfy a similar relation.

To obtain the spectrometer slit function f'(x) the two water vapour absorption lines at 315.03 cm^{-1} and 335.16 cm^{-1} were used. On extrapolation to zero slit width the two water vapour absorption lines were found to have zero half-width. The observed broadening of these lines, due to the finite slit width of 1.0 mm, is the spectrometer slit function. All runs were done with a 1.0 mm slit width. The slit function at 344 cm^{-1}, the position of the $1s_1 - 2p_0$ absorption line, was obtained by extrapolation of the data at 315 cm^{-1} and 335 cm^{-1}.

The observed absorption line profiles of the arsenic-doped silicon and the profiles of the water vapour absorption were found to be neither Lorentzian nor Gaussian; consequently, they were fitted to a Voigt function (H.C. Van de Hulst and J.J.M. Reesinick). These functions are defined as the convolution integral between a Gaussian and Lorentzian function. They may be used to fit any profile which lies between a Lorentzian and a Gaussian curve. If the observed line shape and the spectrometer slit function are both taken to be Voigt functions, then, the true line profile is also a Voigt function Eq. (II-4).

One may thus write,

the observed line shape

$$f(x) = M \int_{-\infty}^{\infty} \frac{\exp[-(y/\beta_2)^2]}{1+[(x-y)/\beta_1]^2}\, dy \,, \qquad \text{II-9}$$

the slit function

$$f'(x) = M' \int_{-\infty}^{\infty} \frac{\exp[-(y/\beta_2')^2]}{1+[(x-y)/\beta_1']^2}\, dy \,, \qquad \text{II-10}$$

the true line shape

$$f''(x) = M'' \int_{-\infty}^{\infty} \frac{\exp[-(y/\beta_2'')^2]}{1+[(x-y)/\beta_1'']^2}\, dy \,, \qquad \text{II-11}$$

where M, M', and M'' are constants. The Voigt function parameters β_1 and β_2 satisfy the relations,

$$\beta_1 = \beta_1' + \beta_1'' \,, \qquad \text{II-12}$$

$$\beta_2^2 = \beta_2'^2 + \beta_2''^2 \,. \qquad \text{II-13}$$

The parameters for the slit function and the observed line shape were calculated using the tables of H. C. Van de Hulst and J.J.M. Reesinick (K. Colbow, Ph.D. thesis 1962)

The parameters for the two water vapour absorption lines were the same within experimental error,

$$\beta_1' = .060 \pm .01 \qquad \beta_2'^2 = 0.020 \pm .005 \qquad \text{II-14}$$

Hence, these were the parameters used for the slit function at 344 cm^{-1}. To obtain the parameters for the true line shape, one must use the relations, Eq. (II-12) and Eq. (II-13). The values of the parameter β_2^2 for the observed line shapes were within error the same as $\beta_2'^2$, giving a $\beta_2''^2$ equal to zero. Thus, the true line shape in all cases is pure Lorentzian, and its half-width may be obtained from the relation,

$$h = 2\beta_1'' = 2(\beta_1 - \beta_1'), \qquad \text{II-15}$$

which accounts for the spectrometer broadening. In Fig. 3 the temperature dependence of the true absorption line half-widths is given for four impurity concentrations. The mean of the two curves with impurity concentrations of 1.7×10^{15} cm^{-3} and 9.0×10^{14} (Fig. 3) will be referred to as corresponding to an impurity concentration of 1.0×10^{15} cm^{-3}, in the following analysis of broadening.

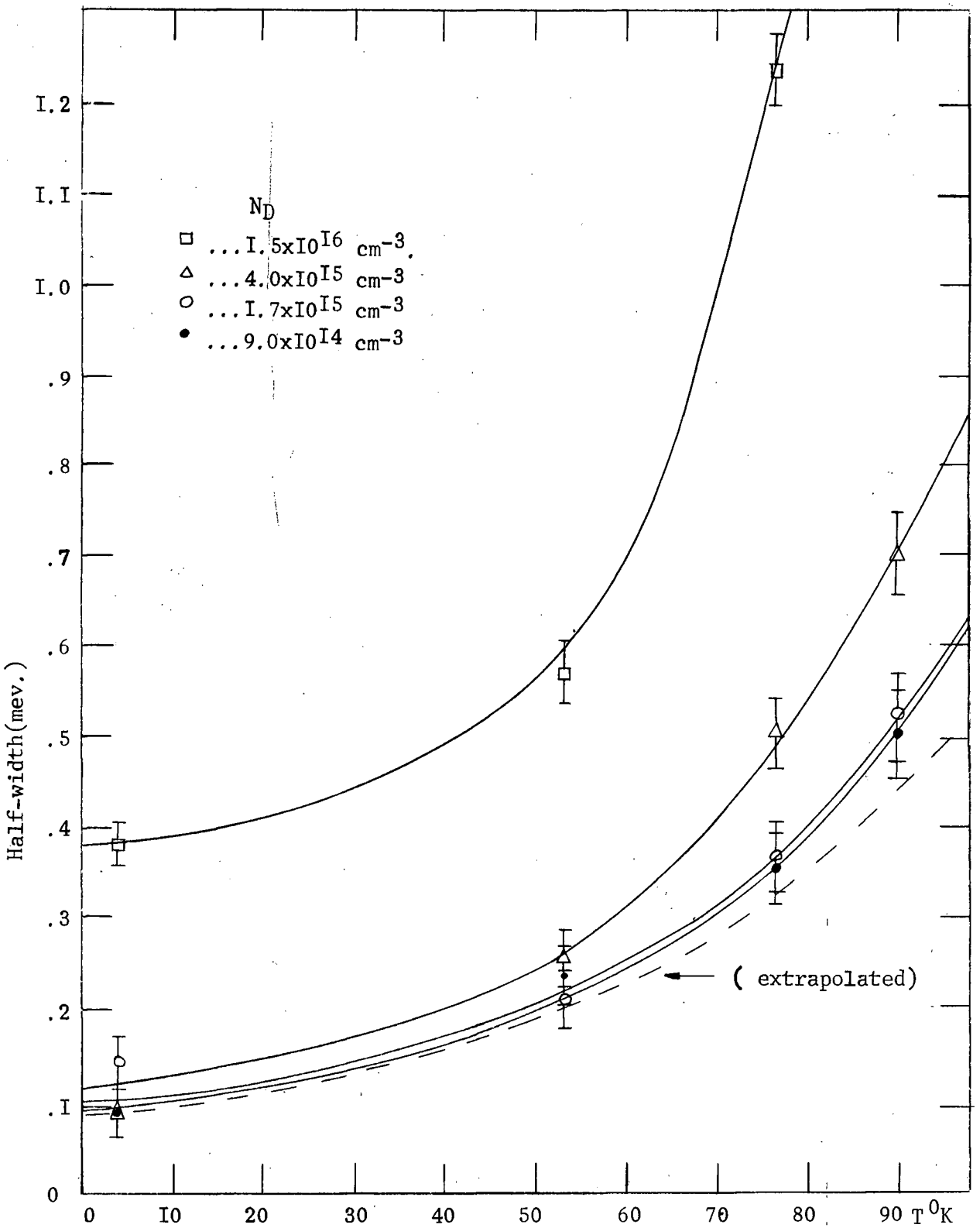

FIG. 3. The temperature dependence of the true absorption line (IS_{I}-$2P_{0}$) half-width of arsenic-doped silicon. The impurity concentrations N_D are $I.5\times10^{16}cm^{-3}$, $4.0\times10^{15}cm^{-3}$, $I.7\times10^{15}cm^{-3}$, $9.0\times10^{14}cm^{-3}$, and zero concentration(extrapolated).

CHAPTER III

1. Introduction to Analysis of Broadening

It is proposed that there are four specific mechanisms which broaden the absorption lines of arsenic-doped silicon; concentration broadening, due to the presence of neighbouring arsenic impurities; phonon broadening, introduced through phonon-electron interaction; strain broadening, caused by dislocations modifying the crystal structure; and, statistical Stark broadening produced by the electric field set up at unionized impurity sites by ionized impurities.

In order to separate the magnitude of each of the above effects, the following assumptions are made. Each mechanism is assumed independent of any other. The line shape produced by each of the four interactions is assumed to be Lorentzian. Under these assumptions, simple addition of these contributing half-widths will give the half-width of the true line shape (Eq. II-4, II-13).

To obtain the phonon and strain broadening contribution, the half-widths for each temperature were extrapolated to zero concentration of impurities (Fig. 4). The values of half-width at zero concentration represent only the strain and phonon broadening. The line width at zero concentration is that attributed to only one impurity atom. Hence, the statistical Stark broadening and concentration broadening is zero, since, they both depend on the effect of many impurity atoms. In Fig. 5, a plot of zero concentration half-widths versus temperature is given. The strain broadening is assumed temperature and impurity concentration independent and is

represented by a dashed line. This is explained in section 4. The remaining temperature dependent broadening, due to electron-phonon interaction is explained in section 5.

To obtain the concentration and statistical Stark broadening, the phonon and strain broadening (zero concentration half-widths) contribution to the true half-width were subtracted. The remaining half-width versus temperature (Fig. 6) represents statistical Stark and concentration broadening. At $0^{o}K$ (Fig. 6), the half-width for a given impurity concentration is due only to concentration broadening; since, there are no ionized impurities at $0^{o}K$, hence no statistical Stark effect. The concentration broadening half-width is assumed temperature independent and is represented by a dashed line. Concentration broadening is explained in section 3. The remaining half-width due to the statistical Stark effect is now explained.

2. Statistical Stark Broadening

(i) Effect of Ionized Impurities

A semiconductor with a random distribution of N_i ionized and $N_D - N_i$ neutral donor impurities per cm^3 will have an electric field at an absorping neutral impurity site dependent on the number and position of the surrounding ionized impurities. Broadening of the resultant absorption lines may thus be caused by first order Stark splitting or second order Stark shifts.

Let us suppose that the distribution of intensity of absorption for one neutral impurity which is in an electric field F is given by $I(F,\omega)$;

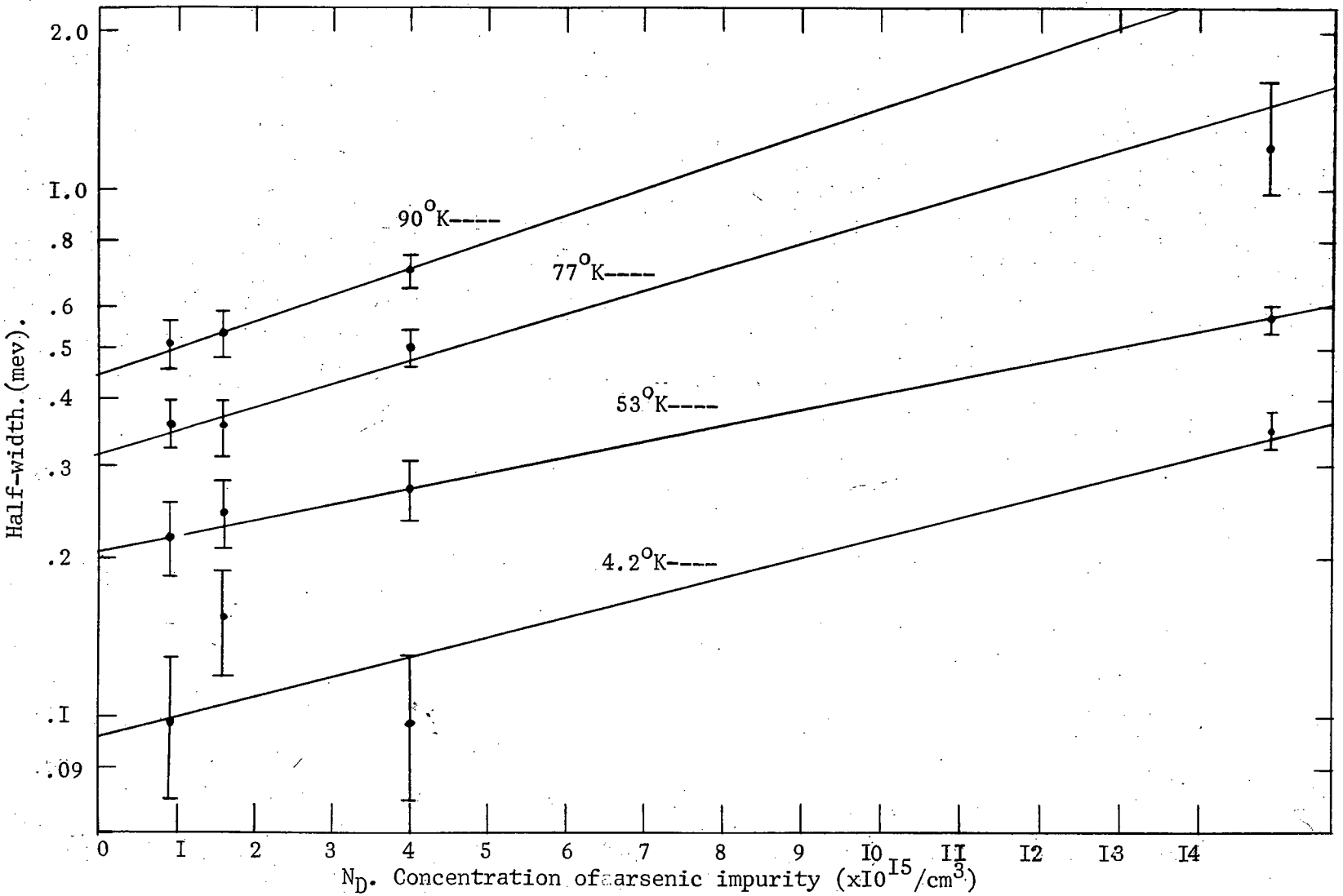

FIG.4. Extrapolation of the half-widths at four temperatures 4.2°K.,53°K.,77°K., and 90°K. to zero concentration half-width. (half-width , log. scale)

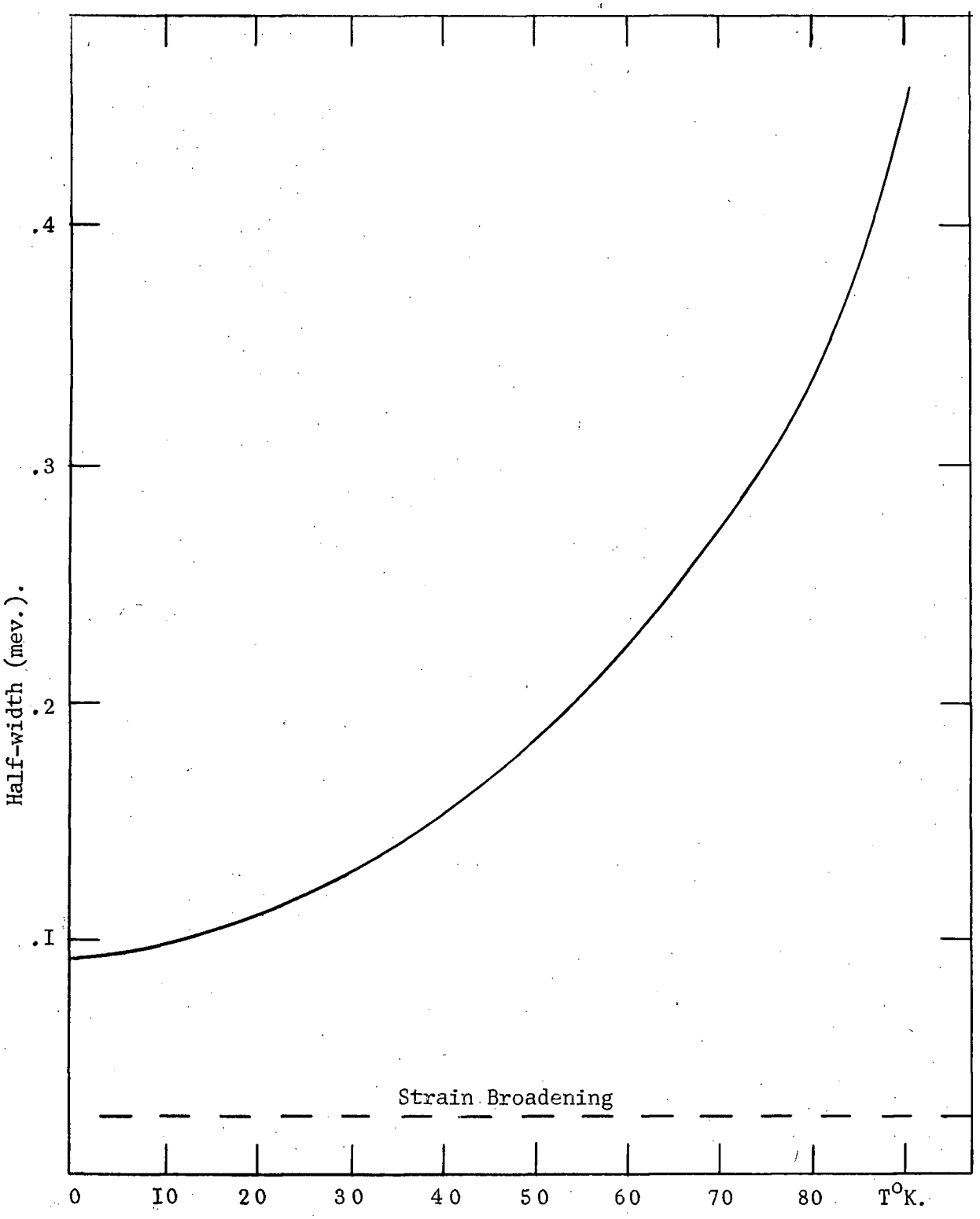

FIG.5. Extrapolated zero concentration half-widths represent phonon and strain broadening . Phonon broadening found by subtracting strain portion.

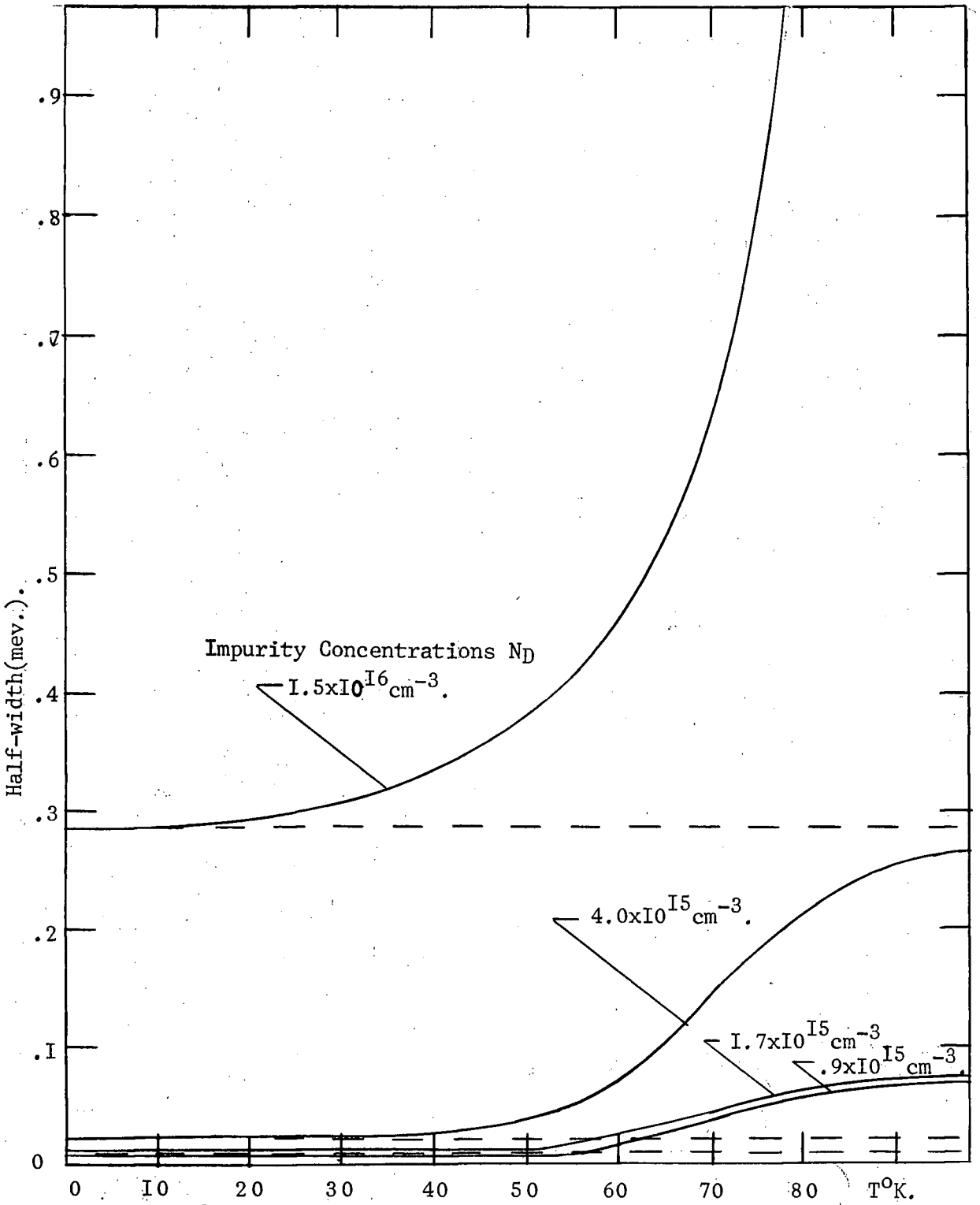

FIG.6. Half-width minus zero concentration half-width (extrapolated). Dashed lines represent concentration broadening ;remainder is statistical Stark broadening. Concentration broadening starts at an impurity concentration of $4.0xI0^{I5}cm^{-3}$.

then in order to obtain the total intensity distribution in the Stark broadened line one must integrate over all such distributions weighted by the probability of the distribution occuring

$$I(\Delta\omega)\, d\omega = d\omega \int_0^\infty I(F,\omega)\, W(F)\, dF. \qquad \text{III-1}$$

Here W(F) is the field strength probability function which has been studied by Holtsmark (1919, 1924) and others in connection with gravitational problems and pressure in gas. Each component of the statistically Stark broadened absorption line will be treated as a sharp line. $I(F,\omega)$ will be replaced by a delta function and thus W(F) will give directly the line shape $I(\Delta\omega)$ due to statistical Stark broadening.

The problem is finding the probability of a frequency displacement $\Delta\omega$ lying between $\Delta\omega$ and $\Delta\omega + d\Delta\omega$. As justified by K. Colbow, (Ph.D. Thesis 1962) only the upper level in the transition will be considered as displaced either by the linear or quadratic Stark effect.

Now the probability of a certain frequency displacement due to the surrounding impurities is related to the probability of a certain electric field at the absorbing impurity. This depends on the probability of finding another impurity at a distance r from the absorbing impurity. Since $I(F,\omega)$ in Eq. (III-1) is taken to be a delta function, the probability function for a frequency displacement between $\Delta\omega$ and $\Delta\omega + d\Delta\omega$ will give directly the desired line shape of the absorption line.

The probability function for a frequency displacement using the simple approximation of considering only the effect of the nearest ionized

neighbour to a neutral impurity site was shown by Konrad Colbow (1962) to be :

for a linear Stark splitting ($\Delta\omega = s F$, $\Delta\omega_0 = s F_0$)

$$I(\Delta\omega) = \frac{s}{|s|} (3/2\, \Delta\omega)(\Delta\omega_0/\Delta\omega)^{3/2} \exp[-(\Delta\omega_0/\Delta\omega)^{3/2}] \qquad \text{III-2}$$

for a quadratic Stark shift ($\Delta\omega = t F^2$, $\Delta\omega_0 = t F_0^2$)

$$I(\Delta\omega) = \frac{t}{|t|} (3/4\, \Delta\omega)(\Delta\omega_0/\Delta\omega)^{3/4} \exp[-(\Delta\omega_0/\Delta\omega)^{3/4}] \qquad \text{III-3}$$

Here the field at the neutral impurity site is given by $F = (e/4\pi\epsilon) r^{-2}$ and t and s are both constants. The field at the mean spacing r_0 defined by

$$(4\pi/3) r_0^3 = 1/N_i \qquad \text{III-4}$$

is given by

$$F_0 = (e/4\pi\epsilon) r_0^{-2} \qquad \text{III-5}$$

For the linear Stark splitting two peaks corresponding to positive and negative s are obtained from Eq. II-2. Depending on the specific energy level structure, the t associated with quadratic Stark shift can be either positive or negative for any given energy level. This nearest neighbour approximation is the binary form of the Holtsmark theory.

In the work of Holtsmark (1919, 1924) and others the intensity distribution due to the co-operative effect of many ions has been obtained. Review articles on this field have been written by Chandrasekhar (1943), Breene Jr. (1957), and Margeneau and Lewis 1959).

The field F at the neutral impurity site is written as the vector sum of the fields of the many ionized impurities surrounding it

$$F = |\Sigma \vec{F}_n| \qquad \text{III-6}$$

The distribution function W(F) calculation is carried out in a configuration space of 3N dimensions.

Holtsmark obtains the function

$$W(\beta) = 2(2/\pi\beta)\int_0^\infty v \sin v \exp[-(v/\beta)^{3/2}]\,dv \qquad \text{III-7}$$

$$= \begin{cases} 4/3\pi\beta^2(1 - 0.463\beta^2 + 0.1227\beta^4 + \cdots) & \beta \text{ small} \\ 1.496\,\beta^{-5/2}(1 + 5.107\beta^{-3/2} + 1.493\beta^{-3} + \cdots) & \beta \text{ large} \end{cases}$$

where $\beta = F/F_o$

In the Binary theory F_o was defined by

$$F_o = (e/4\pi\epsilon) r_o^{-2} = (e/4\pi\epsilon)[4\pi/3N_i]^{2/3} \qquad \text{III-8}$$
$$= 2.60\,(e/4\pi\epsilon) N_i^{2/3}$$

The many ion calculation gives nearly the same parameter.

$$F_o = 2.61\,(e/4\pi\epsilon) N_i^{2/3} \qquad \text{III-9}$$

(ii) The Effect of Screening

When the crystal contains N_i ionized impurities per cm^3, there will also be an equal number $n = N_i$ of free electrons, the influence of which has been neglected so far. The free electrons screen the electric field of the ionized impurities seen by the neutral impurities. The effect of these free electrons may be approximated by using a screened coulomb potential of the form

$$U = (e/4\pi\epsilon)\frac{1}{r} e^{-r/\lambda} \qquad \text{III-10}$$

Here λ is the Debye-Hückel (1923) screening length. In classical statistics

$$\lambda = [kT/4\pi ne^2]^{1/2} \qquad \text{III-11}$$

k being the Boltzmann constant.

Differentiating the expression for U in Eq. (III-10) one obtains the screened coulomb field

$$F = (e\vec{r}/4\pi r^3)[(\tfrac{1}{r})+(\tfrac{1}{\lambda})]e^{-r/\lambda} \qquad \text{III-12}$$

This replaces the simple coulomb field in the nearest neighbour approximation. Using the same approach as Ecker (1957) to simplify the problem, $\vec{F}$ has been approximated by

$$\vec{F} = \begin{cases} e\vec{r}/4\pi\epsilon r^3 & \text{if } r < \lambda \\ 0 & \text{if } r \geq \lambda \end{cases} \qquad \text{III-13}$$

Ecker has calculated the field distribution $W(\beta)$ Fig. 7 which is applicable to a neutral impurity site for various screening parameters σ. The screening parameter, being related to λ by

$$\sigma = (4\pi\lambda^3/3)N_i = 1/6\,\pi^{-1/2}(kT/e^2)^{3/2}n^{-1/2} \qquad \text{III-14}$$

has the physical meaning of giving the number of ionized impurities within the Debye radius. As λ goes to infinity Ecker's curve for $\sigma = \infty$ becomes Holtsmark's distribution. From these curves one can obtain the half-width $h(\beta)$ of the field distribution for various screening parameters σ. These have been obtained in Fig. 8. The dependence of screening parameter, σ, on temperature for three concentrations of impurities is shown in Fig. 9. The screening parameter was calculated using Eq. (III-14) and Fig. 10.

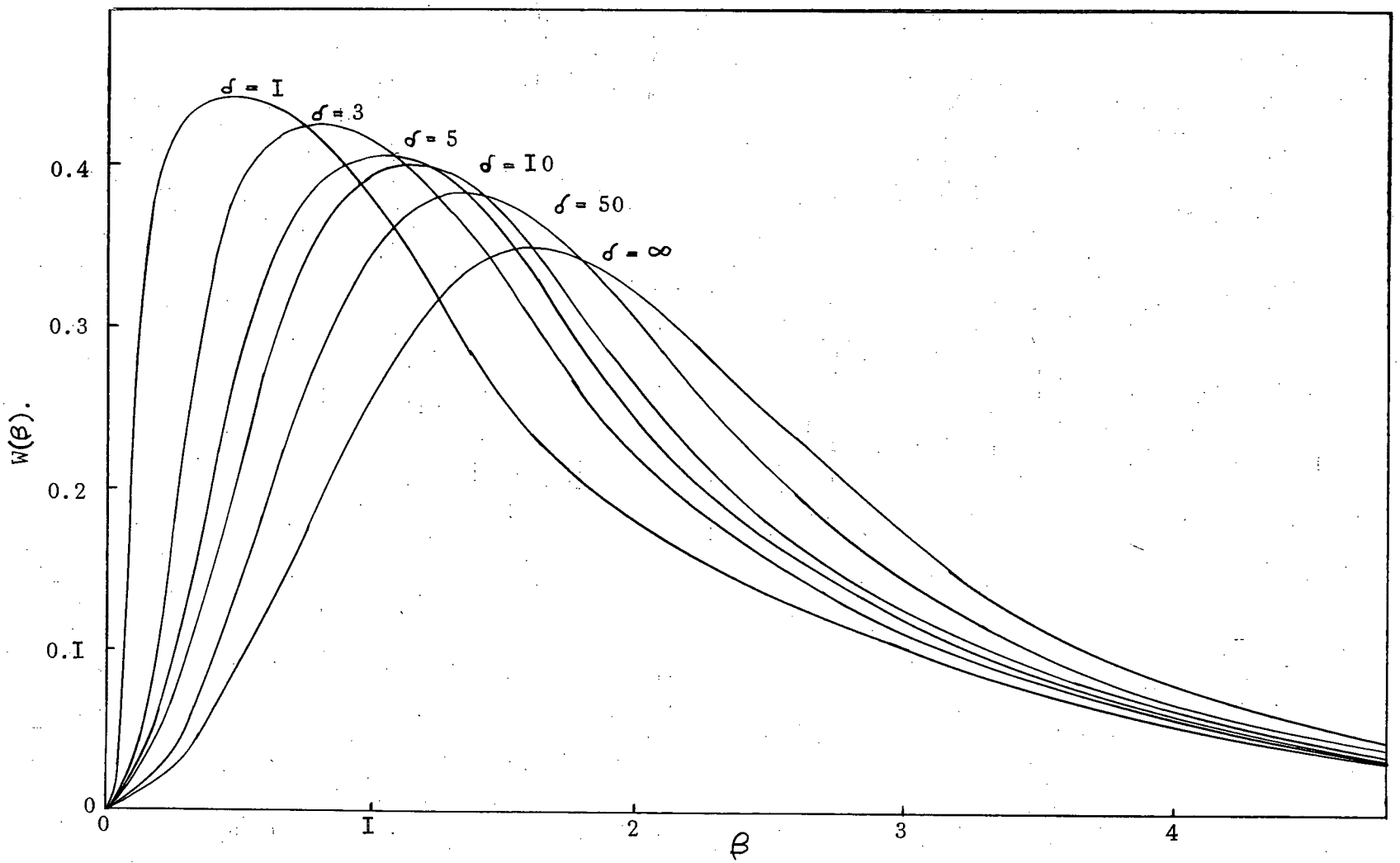

FIG.7. Field distribution, $W(\beta)$ for various values of the screening parameter σ. (Ecker I957)

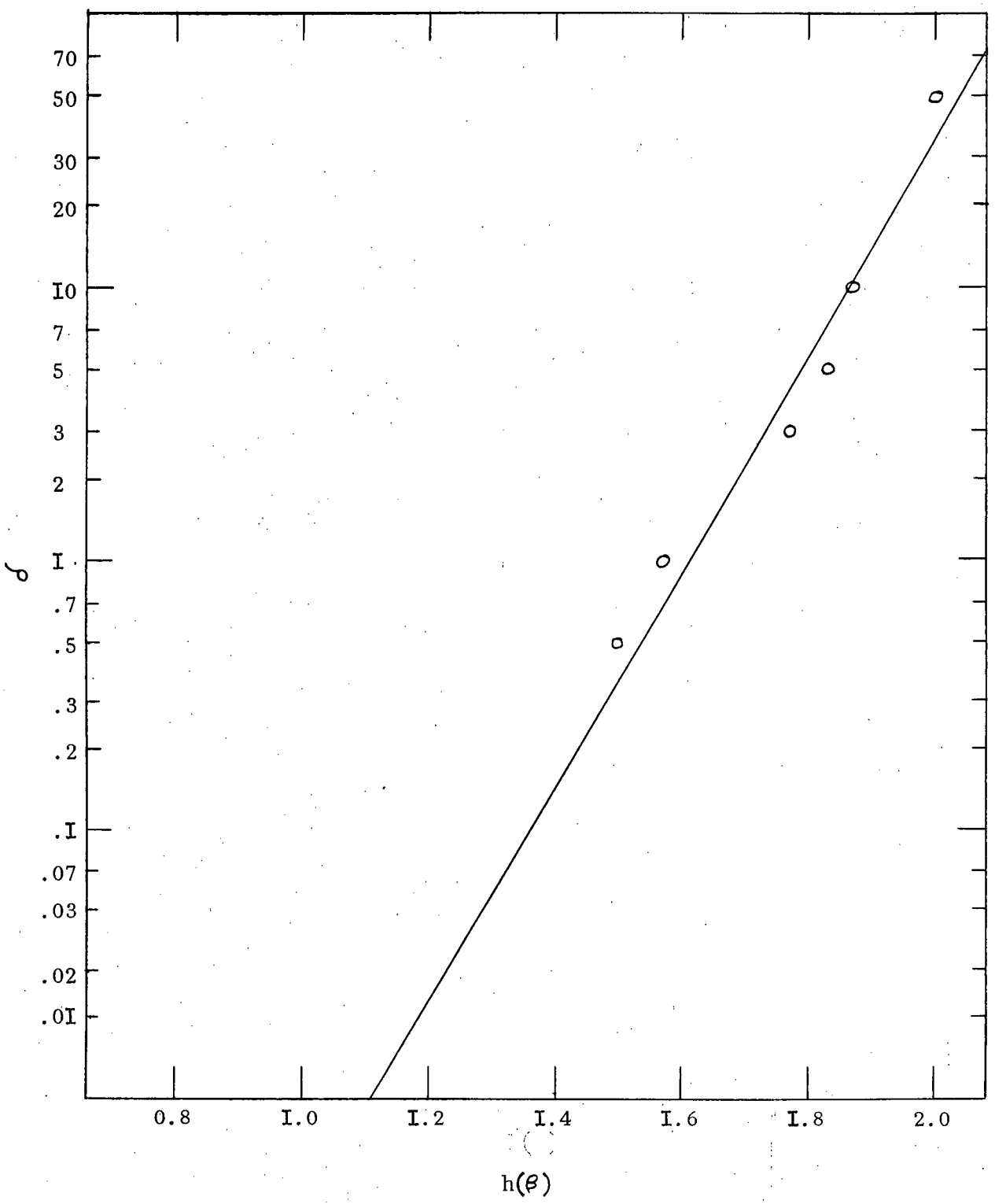

FIG.8. Half-width of the field distribution $h(\beta)$, as a function of screening parameter δ, (logarithmic scale).

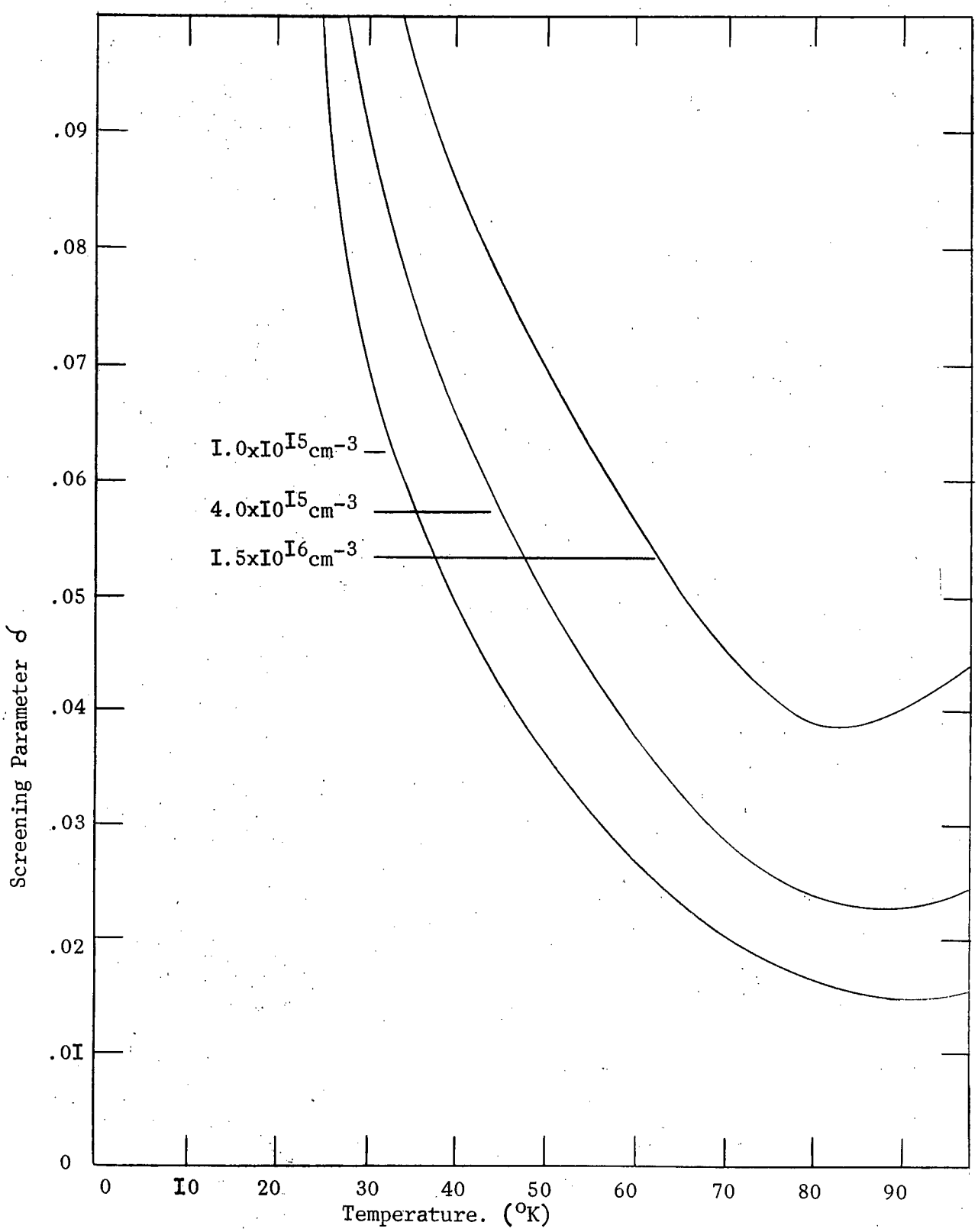

FIG.9. Screening parameter, σ, vs. temperature for arsenic concentrations of i) $I.0xI0^{I5}cm^{-3}$, ii) $4.0xI0^{I5}cm^{-3}$, and iii) $I.5xI0^{I6}cm^{-3}$.

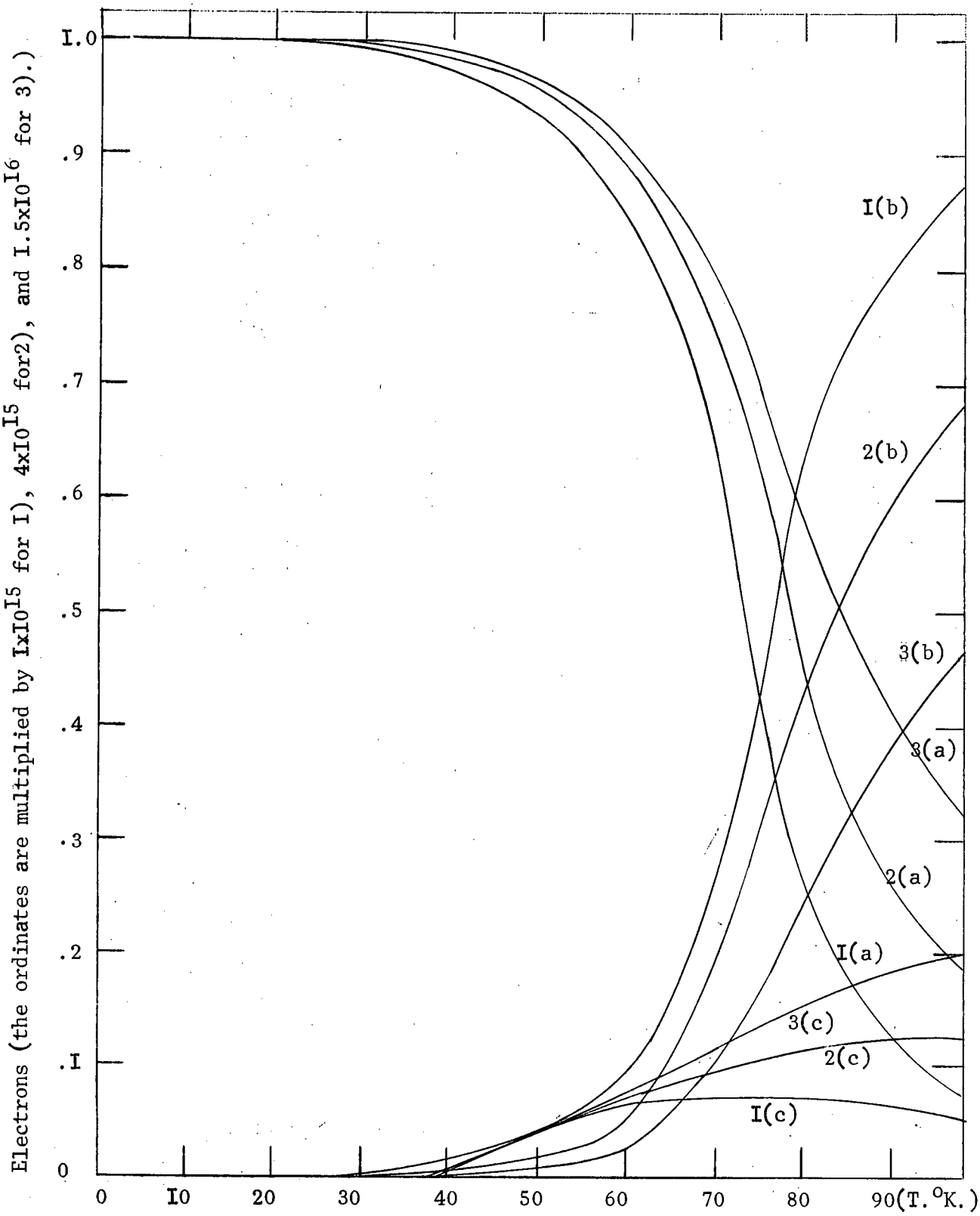

FIG. I0. Distribution of electrons among (a) the ground state, (b) the conduction band, and (c) the excited states. The arsenic concentrations are I) $I.0x10^{15}cm^{-3}$, 2) $4.0x10^{15}cm^{-3}$, and 3)$I.5x10^{16}cm^{-3}$.

which describes the variation of n with temperature and impurity concentration.

(iii) Temperature Dependence of the Half-width due to the Linear and the Quadratic Stark Effect.

For the linear Stark effect

$$\Delta\omega = sF = sF_0\beta \qquad \text{III-15}$$

and hence in units of frequency, the half width of $I(\Delta\omega)$ is given by

$$h_1(\Delta\omega) = s F_0 h(\beta) \qquad \text{III-16}$$

For the quadratic Stark effect

$$\Delta\omega = tF^2 = tF_0\beta^2 \qquad \text{III-17}$$

and hence in units of frequency, the half-width of $I(\Delta\omega)$ is given by

$$h_2(\Delta\omega) = t F_0^2 h^2(\beta) \qquad \text{III-18}$$

Taking for silicon the dielectric constant $\epsilon/\epsilon_0 = 12$ one finds using Eq. III-9

$$F_0 = 2.61(e/4\pi\epsilon)N_i^{2/3} = 3.13\times10^{-8}N_i^{2/3}\ \text{volt cm}^{-1} \qquad \text{III-19}$$

where N_i is in units of cm^{-3}.

Using Eq. III-(16, 18, 19) and Fig. 8 and 9 the curves for $h_1(\Delta\omega)/s$ and $h_2(\Delta\omega)/t$ as a function of temperature for three impurity concentrations have been calculated (Fig. 11 and Fig. 12). This temperature dependence must be compared with the temperature dependence of the half-width of the observed statistical Stark broadening (Fig. 6). It is seen that

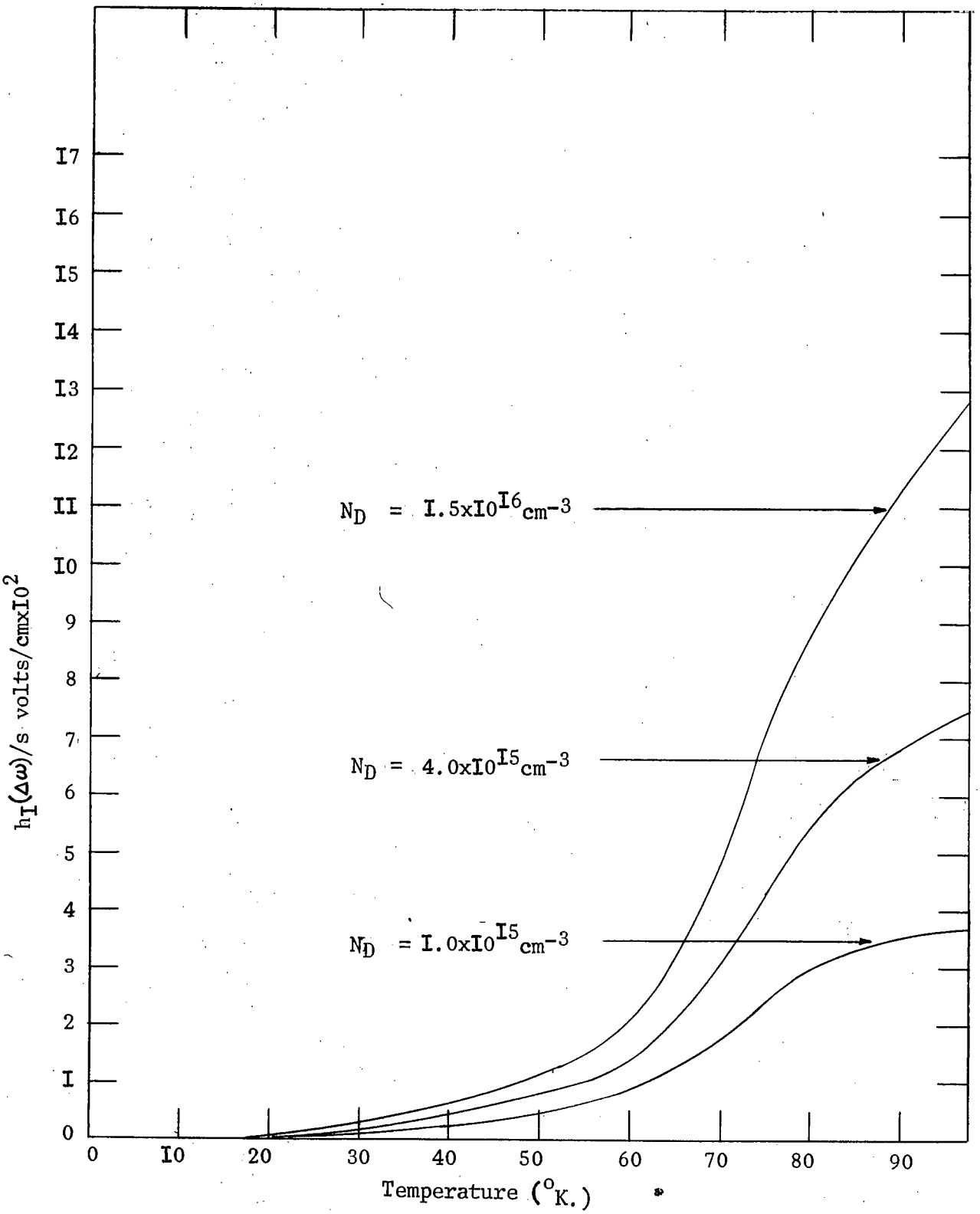

FIG. II. Half-widths in units of the strength parameter s vs. temperature for the linear Stark effect for three arsenic concentrations N_D.

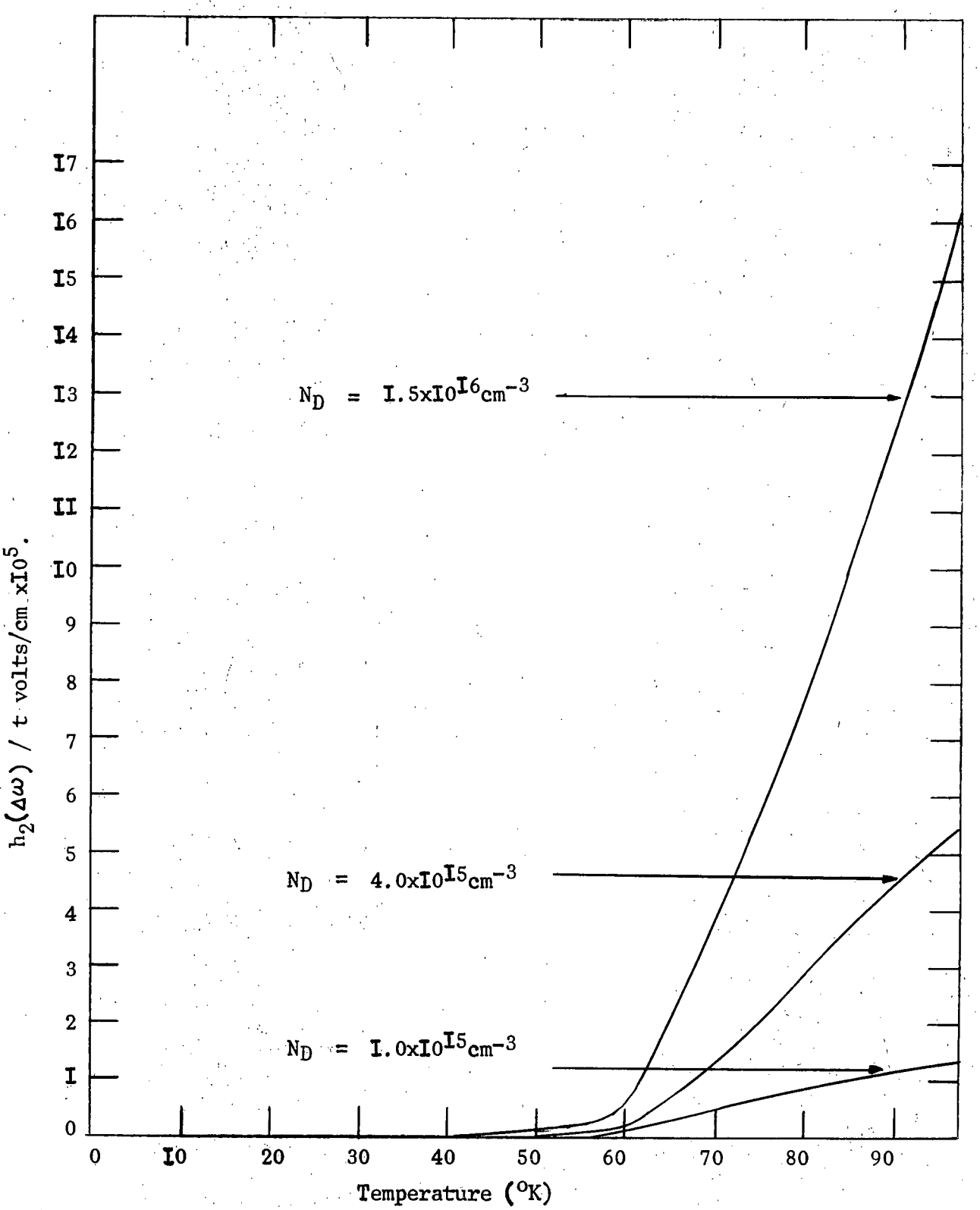

FIG. 12. Half-widths in units of the strength parameter t vs. temperature for the quadratic Stark effect, for three arsenic concentrations N_D.

the quadratic Stark effect's temperature dependence compares more favorably with the observed than does the linear Stark effect's.

It should be noted that only qualitative comparisons can be made, due to uncertainty in the validity of the extrapolation of the screening parameter σ (Fig. 8). It is assumed that the h (β) obtained through the extrapolation does not deviate much from the true value of h (β).

It is interesting to make one quantitative comparison. The experimentally observed statistical Stark broadening increases in the ratio of 1:3.6:11 for respectively the concentrations 1×10^{15}, 4×10^{15} and 1.5×10^{16} impurities/cc at 75°K. The theoretical curves of statistical Stark broadening yield the increase in the ratio of 1:1.8:3.0 for the linear Stark effect and 1:3.2:9.4 for the quadratic Stark effect under the same conditions. This again indicates that the quadratic Stark effect is responsible for the statistical Stark broadening.

Since the effective mass Hamiltonian is invariant under inversion and there are no accidental degeneracies such as the 2_s, 2_p degeneracies in hydrogen, the first order Stark effect vanishes. However, the full Hamiltonian of the impurity problem has only tetrahedral symmetry and is not invariant under inversion. As a result, if the effective mass theory is seriously in error, states belonging to the representations T_1, T_2 and Γ 8 can have an appreciable first order Stark effect. This might possibly be of significance only for the acceptor ground state (Γ 8) in silicon (Kohn 1957). Hence one can say, on the basis of theory and the observed experimental evidence, that only the quadratic Stark broadening occurs in the broadening of donor impurity levels due to the statistical Stark effect.

3. Concentration Broadening

For low impurity concentrations the impurity electron wave functions of one impurity atom are not affected by the presence of other impurity atoms. However, above a certain impurity concentration the wavefunctions overlap appreciabley forming impurity bands. Baltensperger (1953) has predicted the concentrations for the formation of these bands.

For computing the edges of the 1_S, 2_S and 2_P bands, Baltensperger used a simple hydrogenic model in conjunction with the cellular method. The medium is characterized by the effective mass m^* of a conduction electron, and by the dielectric constant K. This involves assuming the validity of the effective mass Schroedinger equation

$$\left(\hbar^2/2m^*\right)\nabla^2\Psi + (e^2/Kr + E_n)\Psi = 0 \qquad \text{III-20}$$

within a sphere of radius r_S related to the density of impurities N_D by

$$(4\pi/3)r_S^3 = 1/N_D \qquad \text{III-21}$$

The general solution of Eq. III-20 has the form

$$\Psi_{nlm} = R_{nl}(r)\,\psi_{lm}(\theta\phi) \qquad \text{III-22}$$

the hydrogen eigenfunctions. The energy is given by

$$E_n = -m^*e^4/2\hbar^2Kn^2 = -e^2/2Ka^*n^2 \qquad \text{III-23}$$

where, in the cellular method, n is to be determined by boundary conditions. a^* is the effective Bohr radius.

Since, with increasing impurity concentration, the 2_p wavefunctions overlap before the 1_S wavefunctions do (Fig. 13) the concentration broadening

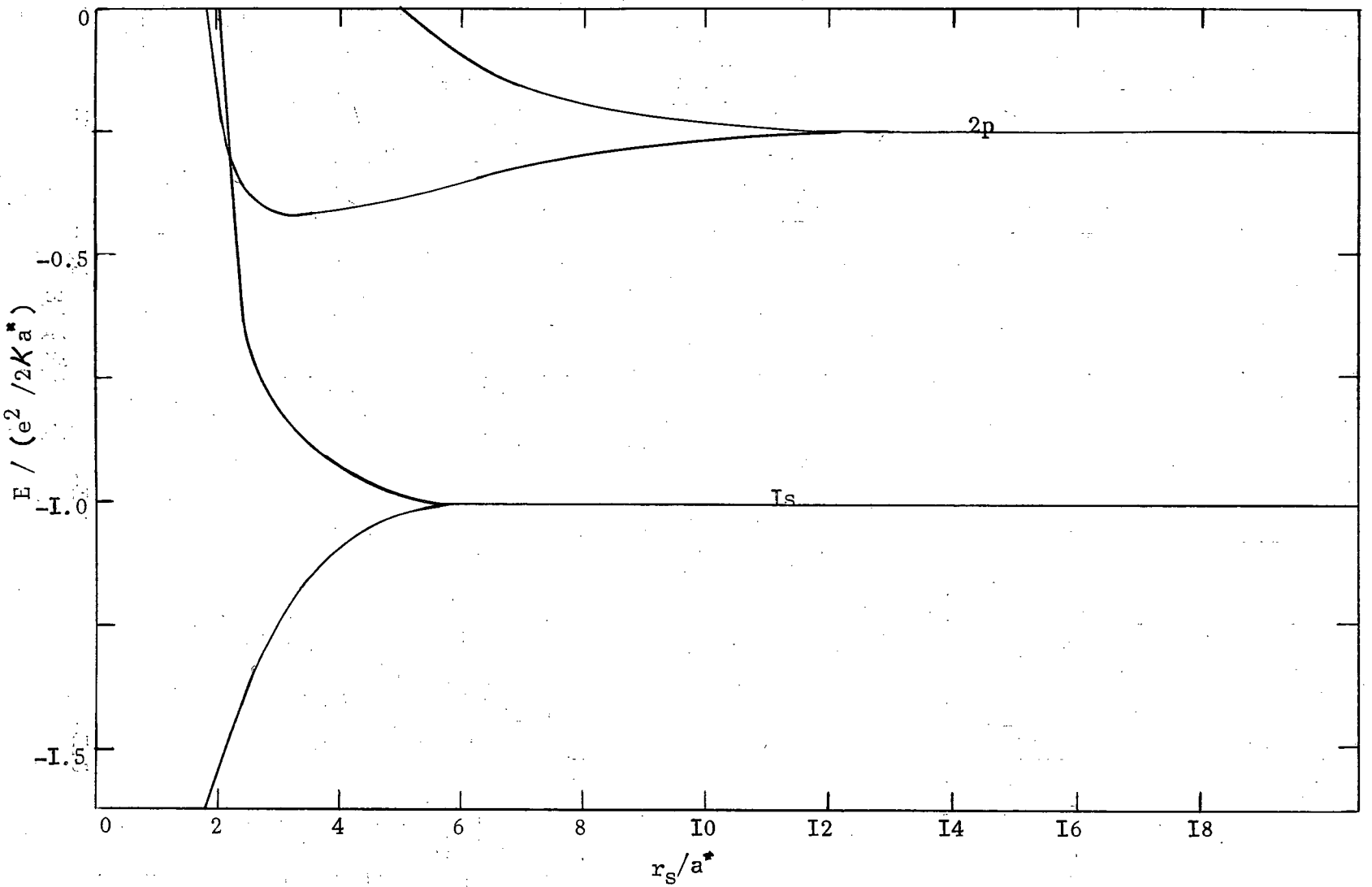

FIG.I3. Broadening of the hydrogenic levels vs. distance between impurities in units of the effective Bohr radius a^* . (Baltensperger I953).

of the transition studied will begin at the concentration for which the 2_p wavefunctions overlap. Baltensperger (Fig. 13) gives the onset of 2_p concentration broadening, as occuring at

$$r_s = 12\,a^* \qquad \text{III-24}$$

Using the observed ionization energy of 11.1 mev. (Bichard and Giles 1962), K = 12 for silicon, and n = 2 in Eq. (III-23), a value of a^* for the 2_p Bohr orbits was found to be 13A°. From Eq. (III-24) and Eq. (III-21), the onset of concentration broadening occurs at an impurity concentration of 6×10^{16} cm^{-3}. If one had calculated a^* from

$$a^* = \hbar^2/m^* e^2 \qquad \text{III-25}$$

the value now obtained for the critical concentration would be greater than 6×10^{16} cm^{-3}. The observed onset of concentration broadening occured between concentrations of 5×10^{15} cm^{-3} and 1×10^{16} cm^{-3} (Fig. 6) which is in closer agreement with the former theoretical estimate. The latter method, for calculating a^*, was not used since it did not lead to the correct ionization energies.

Baltensperger assumes that the impurities form a regular close packed lattice, to facilitate his calculations. A more reasonable arrangement of the impurities might be a random one. K. Colbow (1963) has shown that a random arrangement of impurities decreases the effective radius by a factor of 0.7. Also in this case the critical concentration becomes 2×10^{16} cm^{-3}, in better agreement with the observations.

4. Strain Broadening

For arsenic-doped silicon the optically active excited levels belong to the vector representation T_1 of the tetrahedral group. They are threefold degenerate in the absense of strains. For a shear strain s, arising from internal dislocations, the degeneracy of the levels are split (Kohn 1957) by an amount

$$\Delta E = S \epsilon \qquad \text{III-26}$$

Hence, S is the shear strain and ϵ the shear deformation potential of silicon. The shear strain is given by Kohn as

$$S = (\sqrt{n}) \times 10^{-8} \text{ cm.}, \qquad \text{III-27}$$

where n is the dislocation density per cm^2.

For the ground state the first order shift vanishes from general symmetry considerations. The second order energy shift is given by

$$\delta E^{(i)} = -S^2 \epsilon^2 / \Delta \qquad \text{III-28}$$

where $\Delta = 10^{-3}$ ev (Kohn 1957).

The silicon used has a dislocation density of 5×10^4 giving rise to a strain of 2×10^{-6}. Using a shear deformation potential, calculated to be 11 ± 1 (Wilson, D.K. and Feher 1961), gives a splitting of 12×10^{-6} ev. and a negligble ground state shift. The strain broadening will be of the order of .022 mev. This value was subtracted from the zero concentration half-width. The remainder is due to phonon broadening.

5. Phonon Broadening

Consider the electron of a hydrogen-like impurity atom, being excited from the ground state α to an excited state β. This electron may

return directly to the ground state by radiating a photon. However, there is a probability that the electron can be excited to another state λ by the absorption or emission of a phonon, and return to the ground state via phonon emission. This mode of de-excitation decreases the lifetime of the excited state β, and hence contributes to the energy half-width. This is called phonon broadening.

The theory of Nishikawa (1962) gives the zero phonon half-width broadening of an excited state β due to another excited state λ as

$$\Delta\omega_\lambda = (\epsilon^2/v^2 a^* \rho 2\pi) y_{\beta\lambda} [\overline{|\Theta_{\beta\lambda}(\vec{q})|^2}]_{q=y/a^*} \times \begin{cases} 1+\gamma : T_\beta > T_\lambda \\ \gamma : T_\beta < T_\lambda \end{cases} \qquad \text{III-29}$$

where

$$y_{\beta\lambda} = |T_\beta - T_\lambda| a^*/\hbar v \qquad \text{III-30}$$

$$\gamma = (e^{T_c/T} - 1)^{-1} \qquad \text{III-31}$$

and

$$T_c = \hbar v y_{\beta\lambda}/a^* k \qquad \text{III-32}$$

is the characteristic temperature, above which the half-width starts increasing

$$\Theta_{\beta\lambda}(\vec{q}) = \int d\vec{r}\; F_\beta(\vec{r})^* F_\lambda(\vec{r}) e^{i\vec{q}\cdot\vec{r}} \qquad \text{III-33}$$

$F(\vec{r})$ being the eigenfunction of the unperturbed electronic Hamiltonian, which will be approximated by simple hydrogenic functions.

The other parameters have the following meaning:

$\vec{q}$ = wave number vector of the phonon

v = sound velocity in silicon = 8.3×10^5 cm sec^{-1}

ϵ = deformation potential constant = 15 ev

ρ = density of silicon = 2.33 g cm^{-3}

k = Boltzmann's constant = 1.38×10^{-16} erg deg^{-1}

For the transition studied, the ground state's lifetime is long compared to the excited state's lifetime, allowing one to neglect the ground state's contribution to the half-width. It is seen from Fig. 14, that the half-width of the $1s_1 - 2p_o$ transition starts increasing at a temperature of 25 ± 5^oK. From Eq. (III-29, 30, 31, and 32) this phonon broadening can be attributed to a state lying 3 mev below the $2p_o$ state. Neither an experimentally observed line, nor a theoretically predicted line lies in this region. It is predicted from the effective mass theory (Kohn 1957) that a 2s state lies 2.1 mev above the $2p_o$ state. The same theory predicts the 1s state to lie at 29 ± 1 mev; whereas, the 1s state has been observed to lie at 53.5 mev, a depression of 24.5 mev. Corrections to the effective mass theory have been made by Kohn (1957), which depress the 1s level to agree with the observed energy. It is proposed that if the same correction were applied to the 2s state, a depression of approximately 5.1 mev would be reasonable. Consequently, the 2s level, lying 3 mev below the $2p_o$ level would be in agreement with experiment and theory. For the purpose of simplicity, the $2s_1$, $2s_2$, and $2s_3$ are considered as a six fold degenerate 2s state at 14.1 mev.

From Eq. (III-30,32) the critical temperatures associated with the excited states $2p^{\pm}$ (11.1 mev) and 2s (14.1 mev) are respectively 26^oK and 58^oK. All other states start contributing at higher temperatures. In Fig. 14 the calculated contributions of the 2s and $2p^{\pm}$ states to the half-width of the $1s_1 - 2p_o$ transition are plotted vs temperature. The sum of these contributions is in qualitative agreement with the observed results to 80^oK. At 80^oK, the multiphonon processes and the higher excited states contribute to the observed half-width. Qualitative agreement between the theory of Nishikawa and the results is good.

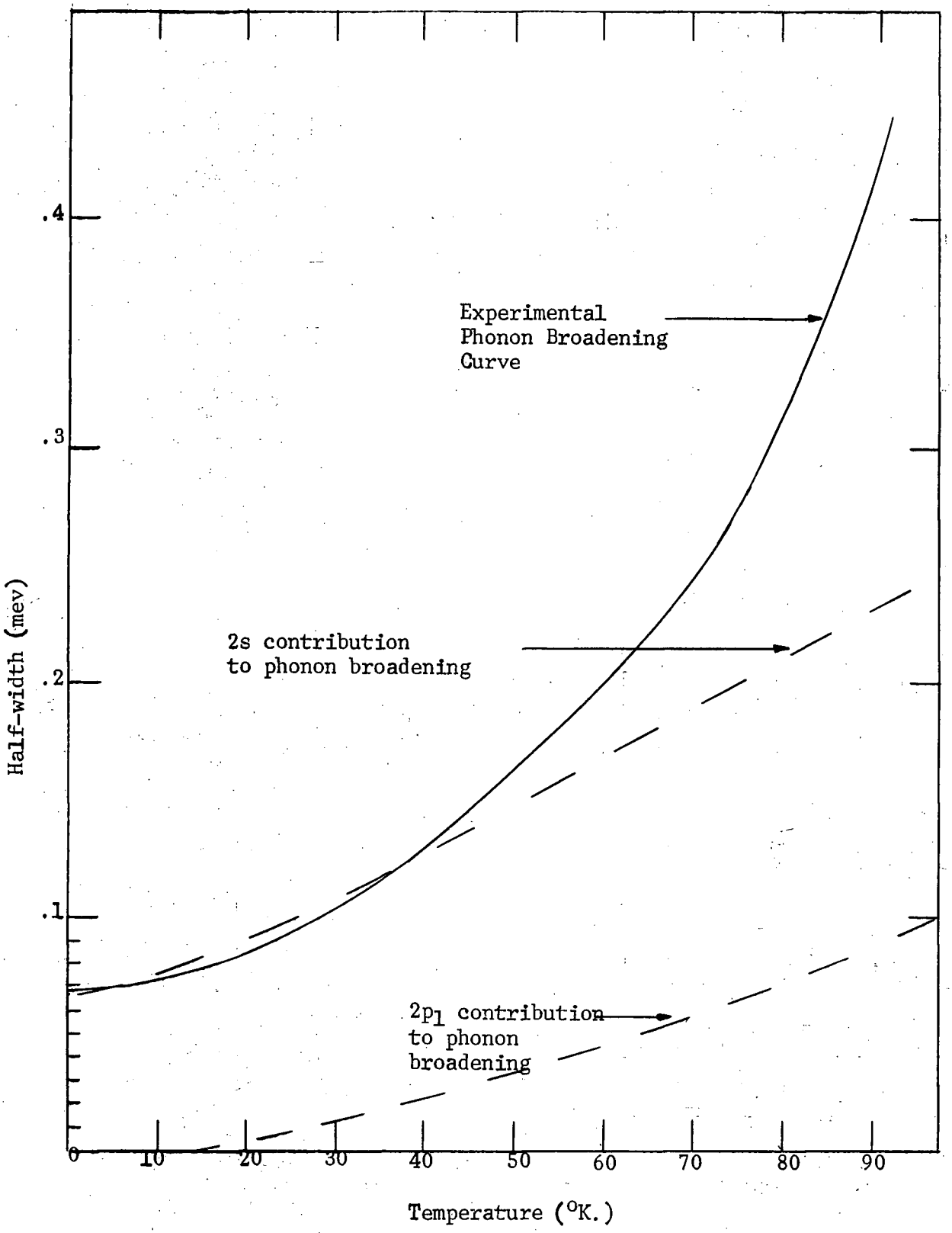

FIG. 14. Extrapolated zero concentration half-widths, with strain broadening removed represents, the phonon broadening of the $1s_1 - 2p_o$ absorption line. The 2s and $2p_o$ contributions are given from theory

6. Temperature Dependence of Line Position

A shift of the centre of the peak with temperature to higher energies was observed. The results indicated that the shift was concentration independent over the impurity concentration range. 9×10^{15} to 4×10^{15} cm^{-3}. The shift for each concentration ($.9 \times 10^{15}$ cm^{-3}, 1.7×10^{15} cm^{-3} and 4.0×10^{15} cm^{-3}) was determined relative to the peak position observed at $4.2^{o}K$ for the three temperatures, $53^{o}K$, $77^{o}K$, and $90^{o}K$ (Fig. 15). It is assumed that the $4.2^{o}K$ peak position is independent of the impurity concentration. To minimize the possibility of any errors in the observed shift for one impurity concentration, consecutive runs at the four temperatures were carried out under identical conditions.

A possible explanation of the temperature dependent shift of peak position might be contained in the electron-phonon interaction as given in the theory of Nishikawa and Barrie (1962).

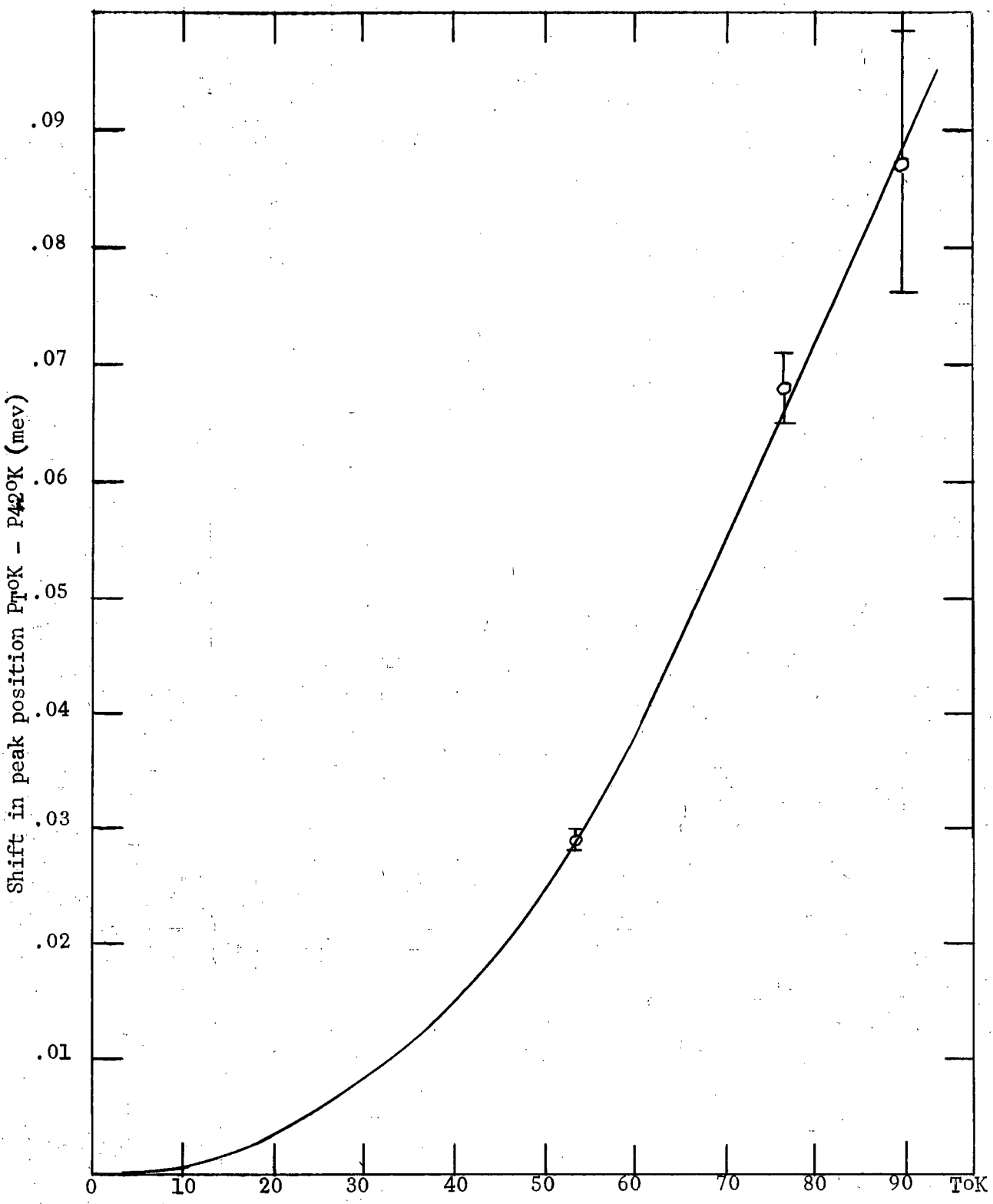

FIG. 15. Shift of peak position with temperature relative to the position of peak at 4.2°K

CHAPTER IV

Conclusion

The study of the arsenic-doped silicon line widths, carried out in this thesis, show that four effects contribute significantly to the true half-widths after line distortion by the finite spectrometer slit width is accounted for. The four effects, contributing significantly to the half-widths, are, statistical Stark broadening, phonon broadening, concentration broadening, and broadening due to internal strains. To the approximation that the absorption lines (corrected for spectrometer broadening) have lorentzian profiles, the half-widths are just the sums of the widths for the four independent broadening mechanisms when each is considered by itself.

In a semiconductor, containing a random distribution of neutral and ionized impurities, different absorbing impurities will be in different electric fields due to the surrounding ionized impurities. From theory (Kohn 1957) these fields W(F) should be expected to give rise to appreciable second-order Stark shifts ($\delta_2 E = t F^2$) of the excited states, resulting in a broadening of the total absorption lines. The contribution to the half-width from this effect was obtained from a knowledge of the field strength probability function W(F). Ecker (1957) computed W(F) including the effect of screening by mobile charge carriers. From an extrapolation of his results and the calculated temperature dependence of the ionized impurity concentration, the calculated quadratic Stark broadening was shown to be characteristic of the rapid rise of the half-width above 50°K.

At very low impurity concentrations, an essential contribution to the half-width is expected to result from the finite lifetime of the excited state due to the electron-phonon interactions. Theoretical calculations show that the half-width for this process is given by

$$h = h_0 / (1 - e^{-T_c/T})$$

The calculated value of h_0 depends on the choice of the characteristic temperature Tc. The best agreement between this theory and the data was obtained for Tc = 26^{o}K and h_0 = 7.0 x 10^{-5} ev. For these values the theory suggests that the lifetime of the state responsible for the absorption line is mostly influenced by a state about 3.0 x 10^{-3} ev. below it. For this reason the 2S state, which is theoretically predicted to be 2.3 mev above the 2_{po} state, is believed to lie 3.0 x 10^{-3} ev below the 2_{po} state. At higher temperatures, the 2s state doesn't fully account for the phonon broadening. The electron-phonon interaction of the other excited states and the multiphonon processes are believed to contribute to broadening at higher temperatures.

In addition, an assumed temperature independent contribution to the half-width of 2.2 x 10^{-5} ev can be expected from internal strains due to dislocations. (corresponding to a dislocation density of about 5 x 10^{4} dislocation lines per cm^2).

A cellular calculation, when modified to fit the assumption of a random distribution of impurities, gives an order of magnitude estimate for the onset of concentration broadening at low temperatures. Broadening of a 2_p state is predicted to start at about 2 x 10^{16} impurities per cm^3, if one replaces the mean spacing (r_s) between impurities by an effective

mean spacing of 0.7 r_s, and takes a^* equal to 13 ^{o}A. This value of a^* gives the experimental binding energy of 11.1 x 10^{-3} ev for this state.

A concentration independent shift in peak position to higher energies was observed with increasing temperature. It is proposed that the electron-phonon interaction, considered in the theory of Nishikawa and Barrie (1962) to explain phonon broadening, could possibly account for this shift, if the temperature dependent electron-phonon interaction matrix-elements were evaluated. (This will be presented in a forth coming paper in C. J. P.).

Appendix A: Distribution of Electrons for an N Type Semiconductor.

In order to calculate the electron distribution we assume that the number of acceptor impurities and free holes is negligible. There are N_D donor impurities and each impurity can accept one electron of either spin or no electron at all.

The density of electrons (Shifrin 1944) in energy state q is given by

$$n_q = N_D q_q \exp\{(E_F - E_q)/kT\} \Big/ 1 + \sum_s q_s \exp[(E_F - E_s)/kT] \qquad \text{A-I}$$

and the density of free carriers is given by

$$n_f = N_c \exp\{(E_F - E_c)/kT \qquad \text{A-2(a)}$$

$$= N_D \Big/ 1 + \sum_s q_s \exp(E_F - E_s)/kT \qquad \text{A-2(b)}$$

assuming that $(E_F - E_c)/KT >> 1$. For $n < 0.4\ N_c$ for A-2(a) (Smith 1958) this approximation holds, as in the case for calculations in this thesis. E_F is the Fermi level, E_c is the energy of the lowest level in the conduction band, E_q is the q th energy level of the impurity spectrum, q_q is the degeneracy of the q th level, E_c is the energy of the lowest level in the conduction band.

The density of states in the conduction band N_c is given by

$$N_c = 2 m_L^{1/2} m_T M_c h^{-3} (2\pi kT)^{3/2} \qquad \text{A-3}$$

where the energy surfaces in silicon are described by ellipsoids of revolution, with effective electron masses being m_L and m_T . M_c is the number of equivalent minima in the conduction band.

To calculate nf, we eliminate $\Sigma_s q_s \exp[(\mu - E_s)/kT]$ between A-2(b) and A-I obtaining

$$n_q = N_D q_q \exp[(E_F - E_q)/kT] \Big/ N_D/n_f \qquad \text{A-4}$$

$$= n_f q_q \exp[(E_F - E_q)/kT]$$

From A-2(a) $\exp(E_F/kT) = (n_f/N_c)\exp(E_c/kT)$

$$n_q = (n_f^2/N_c)\, q_q \exp[(E_c - E_q)/kT] \qquad \text{A-5}$$

Since $\Sigma n_q + n_f = N_D$

$$n_f^2 \Sigma q_q \exp[-E_q/kT]\exp[E_c/kT] + N_c n_f - N_c N_D = 0 \qquad \text{A-6}$$

Take E_c = o as origin and solving for nf

$$n_f = \frac{-N_c \mp \sqrt{N_c^2 + 4N_c N_D \Sigma q_q \exp[-E_q/kT]}}{-n_f^2 \Sigma q_q \exp[-E_q/kT]} \qquad \text{A-7}$$

We now know the number of free carriers.

The bound electrons will be given by

$$n_b = \Sigma n_q = N_D - n_f \qquad \text{A-8}$$

For the excited states, Boltzmann statistics also apply in the temperature range used ($> 60^{o}K.$).

The probability that a state at an energy E_q and of degeneracy q_q is occupied at temperature T is

$$P_q = A\, q_q \exp[E_q/kT] \qquad \text{A-9}$$

Summing over all bound states that are occupied, gives

$$\sum_s P_s = A \sum_s q_s \exp[E_s/kT] = 1 \qquad \text{A-10}$$

therefore,

$$P_q = \frac{q_q \exp[E_q/kT]}{\sum_s q_s \exp[E_s/kT]} \qquad \text{A-11}$$

and

$$n_q = \frac{q_q \exp[E_q/kT]}{\sum_s q_s \exp[E_s/kT]} \cdot n_b \qquad \text{A-12}$$

The series expansion was limited to a few terms. The unwanted terms were eliminated through the criteria

$$\frac{n_2}{n_{q>2}} = \frac{q_2}{q_{q>2}} \exp[(E_2 - E_{q>2})/kT] >> 1 \qquad \text{A-13}$$

BIBLIOGRAPHY

Baltensperger, W. 1953. Phil. Mag. 44, 1355.

Barrie, R. and Nishikawa, K. 1963. Can. J. Phys. 41, 1823.

Bichard, J. and Giles, J. C. 1962. Can. J. Phys. 40, 1480.

Blaine, L. R., Plyler, E. K., and Benedict, W. S. 1962. J. Research NBS-A 66A, 223.

Breene, Jr., R. G. 1957. Rev. Modern Phys. 29, 94.

Burstein, E., Picus, G. S., Henvis, B., and Wallis, R. 1956. J. Phys. Chem. Solids, 1, 65.

Chandrasekhar, S. 1943. Revs. Modern Phys. 15, 1.

Colbow, K. 1963. Ph.D. thesis, University of British Columbia.

Colbow, K. 1963. Can. J. Phys. 41 1801.

Debye, P. and Huckel, E. 1923. Physik. Z. 24, 185.

Ecker, G. 1957. Z. Physick 148, 593; 149, 254.

Holtsmark, J. 1919. Am. Physick, 58, 577, Physick. A. 20, 162.

Holtsmark, J. 1924. Physick Z. 25, 73.

Kohn, N. 1957. Solid State Physics, edited by F. Seitz and D. Turnbull, Vol. 5 (Academic Press, Inc., New York), p.257.

Moss, T. S. 1959. Optical properties of semiconductors (Butterworths, London), p. 14.

Ottensmeyer, P., Giles, J. C., and Bichard, J. W. (to be published)

Shiffrin, K. S. 1944. J. Tech. Phys. Moscow 14, 43.

Smith, R. A. 1958. Semiconductors (Cambridge University Press), P. 80.

Unsold, A. 1955. Physik der Sternatmospharen (Springer-Verlag, Berlin, Gottingen, Heidelberg), Chap. IX.

Van de Hulst, H. C. 1946. Bull. Astron. Inst. Neth. 10, 75.

Van de Hulst, H. C. and Reesinck, J. J. 1947. Astrophys. J. 106, 121.

Voigt, W. 1912. Munch. Ber. 603.

Wilson, D. K. and Feher, G. 1961. Phys. Rev. 124, 1068.